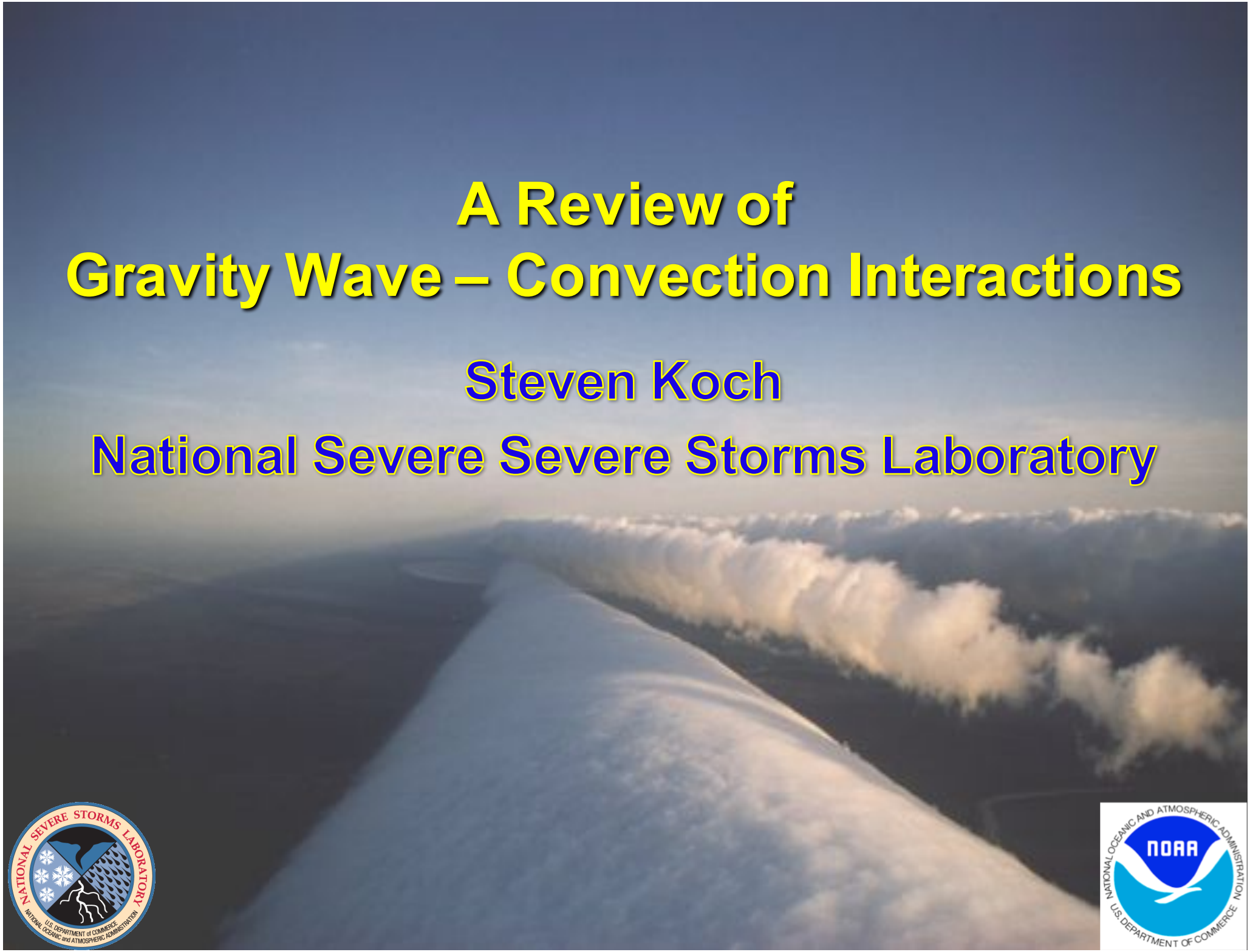

A Review of Gravity Wave – Convection Interactions

Steven Koch

National Severe Severe Storms Laboratory

Convection-Gravity Wave Interactions Theories

Generation of Small-scale Gravity Waves by Deep Convection

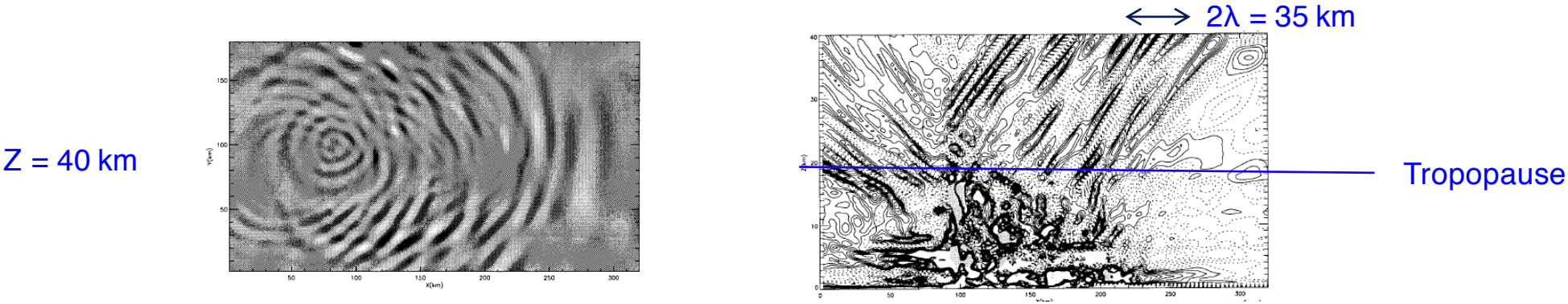

Three popular hypotheses presently:

1. **"Convective Bomb"**
   - Forced by transient, impulsive cloud diabatic heating in a stably stratified atmosphere
   - (Bretherton 1988; Lin et al. 1998; Pandy and Alexander 1999; Beres 2004)

2. **"Moving Mountain"**
   - Transient obstacle effect of updraft in the presence of shear
   - (Clark et al. 1986; Hauf and Clark 1989; Beres et al. 2002)

3. **"Mechanical Oscillator"**
   - Deceleration of convective updrafts as they impinge upon the tropopause and subsequently oscillate about their level of neutral buoyancy, generating waves in the stratosphere
   - (Pierce and Coroniti 1966; Fovell et al. 1992; Lane et al. 2001)

Gravity Wave Generation by Deep Tropospheric, Three-Dimensional Latent Heating

(Beres 2004)

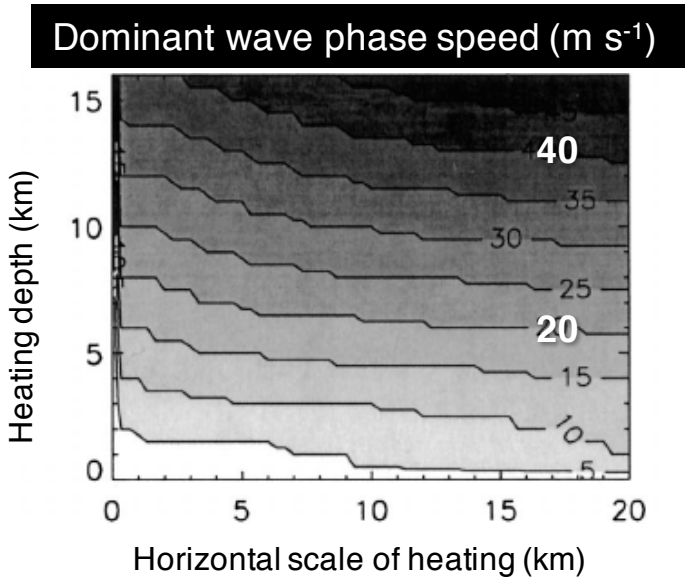

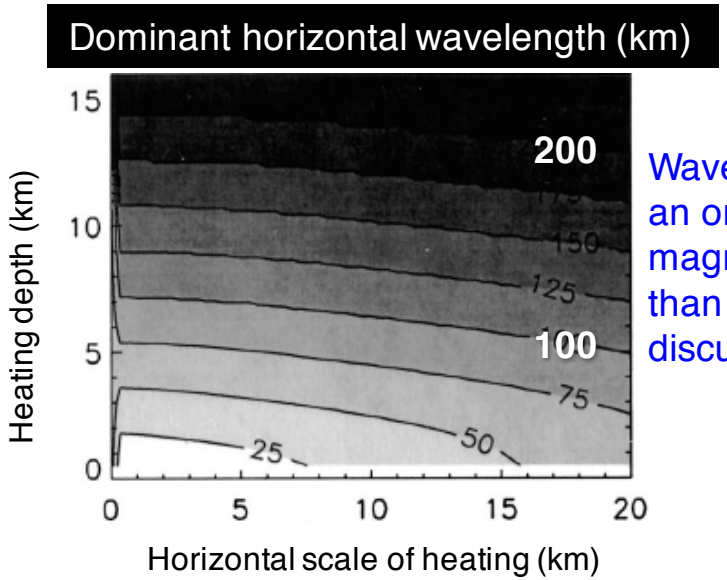

Wavelengths are an order of magnitude larger than those discussed above

$$\left(\frac{\partial}{\partial t}+\bar{U}\frac{\partial}{\partial x}+\bar{V}\frac{\partial}{\partial y}\right)^2\left(\frac{\partial^2}{\partial x^2}+\frac{\partial^2}{\partial y^2}+\frac{\partial^2}{\partial z^2}\right)w'+N^2\left(\frac{\partial^2}{\partial x^2}+\frac{\partial^2}{\partial y^2}\right)w'=\frac{g}{\theta_0}\left(\frac{\partial^2}{\partial x^2}+\frac{\partial^2}{\partial y^2}\right)\dot{Q}$$

1. The dominant wave phase speed increases strongly with increasing **heating depth**, but is rather insensitive to the horizontal scale of the heating.
2. The dominant horizontal wavelength also depends strongly on **heating depth**, and is rather insensitive to the horizontal scale of the heating
3. Convectively generated gravity waves in the stratosphere have a dominant vertical wavelength similar to that of the **depth of tropospheric latent heating**.

Solitary Waves (balance between nonlinearity and dispersion) **generated by Impulsive Convection** (Lin and Goff 1988)

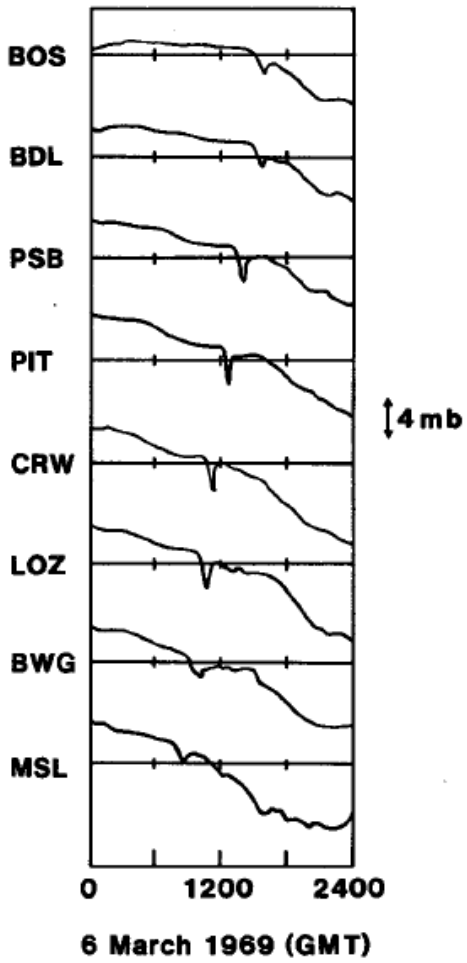

Surface pressure traces for selected stations on 6 March 1969

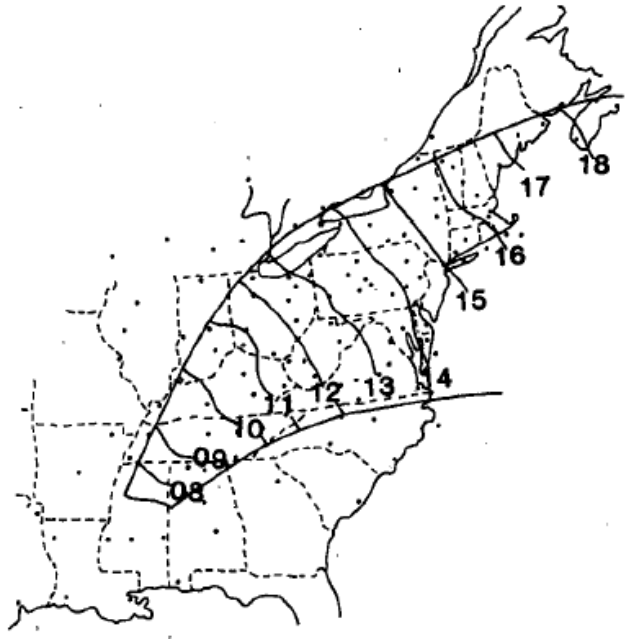

Isochrones of minimum pressure indicating passage of the solitary wave

KdV-type Solitary Wave of Depression

Generated at the inversion when H=5.5 km and phase speed is c_0 = 55 m s^{-1} (observed)

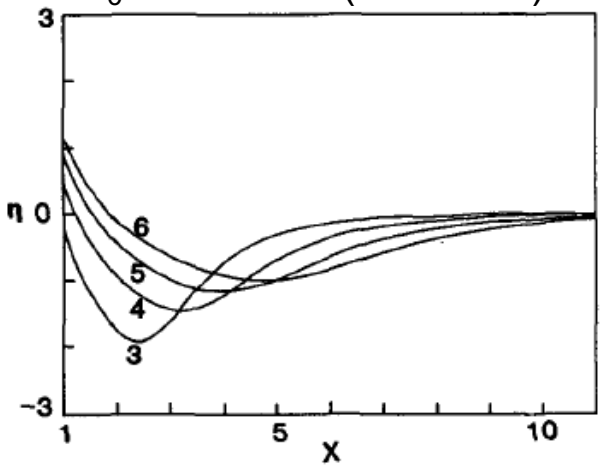

BOD Solitary Wave of Elevation

Generated when inversion height H=1.0 km and phase speed is 10 m s^{-1}

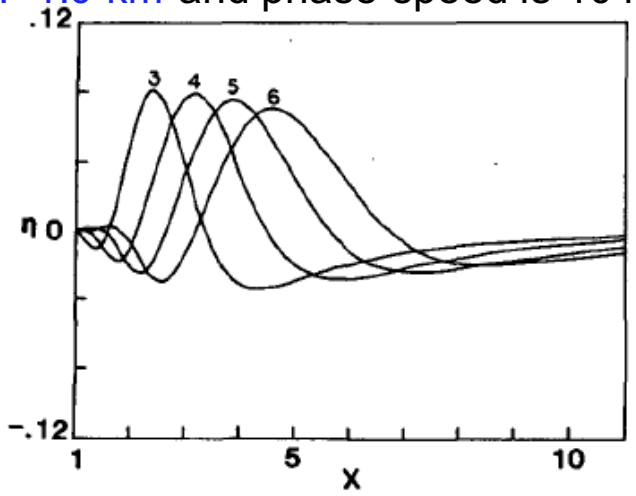

Wave Maintenance Mechanism: Wave-CISK

(Lindzen 1974; Raymond 1975, 1983; Davies 1979; Bolton 1980; Xu and Clark 1984)

Latent Heat Release in active convection acting as a Gaussian heat source

→Generates gravity waves

→Wave-associated low-level moisture convergence

→Convergence forces more convection

→Latent heating (self-sustaining system)

Governing equation for 2D, small amplitude, hydrostatic, inviscid, non-rotating, Boussinesq, quiescent fluid:

$$\frac{\partial^4 w'}{\partial t^2 \partial z^2} + N^2 \frac{\partial^2 w'}{\partial x^2} = \frac{g}{\theta_0} \frac{\partial^2 \dot{Q}}{\partial x^2}$$

Vertical structure equation from Fourier transform of the governing equation:

$$\frac{\partial^2 \hat{w}}{\partial z^2} + \left(\frac{Nk}{\omega} \right)^2 \hat{w} = \frac{Q_0 b k^2}{4\pi\omega^2} e^{-b|k|} \delta(z - z_1)$$

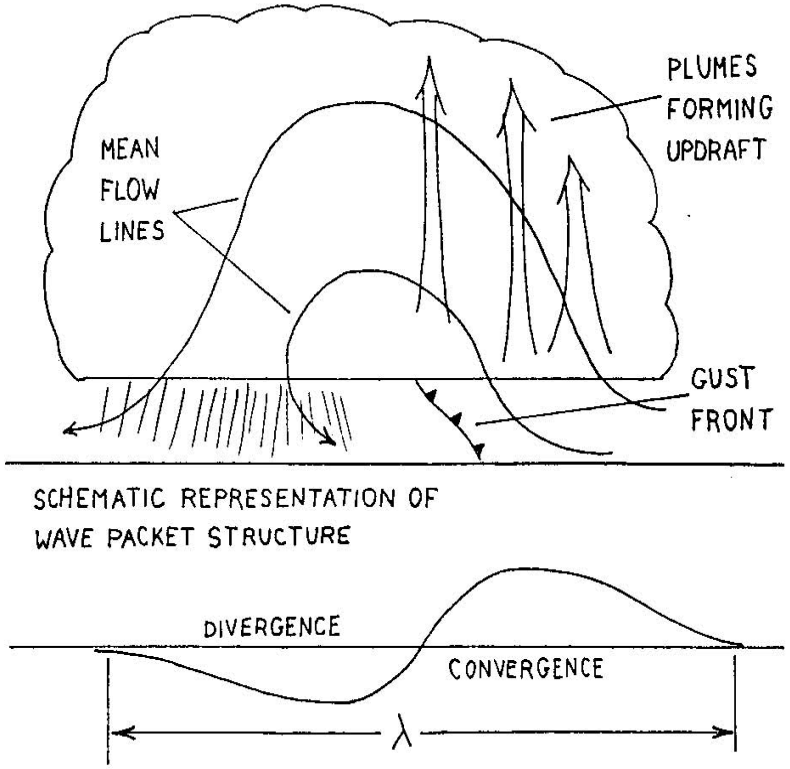

Result: a series of dispersive, progressive waves moving away from the heat source – note sensitivities to scale of Gaussian heat source (b) and wavenumber

Problems with Wave-CISK Theory

1. Sensitivity to heating depth/scale

2. Sensitivity to downdraft mass flux (must exceed updraft)

3. Sensitivity to the particular manner in which convective heating lags updraft in time

4. CISK-driven modes display an instability that increases monotonically with wavenumber unless shear or time-lagged updrafts are introduced

5. Quasi-equilibrium assumption is only valid if the life cycle of convective clouds is negligibly small compared to the convergence forcing, thus the need for imposition of phase lagging in the model

Most commonly observed structures are DUCTED WAVE-CISK MODES

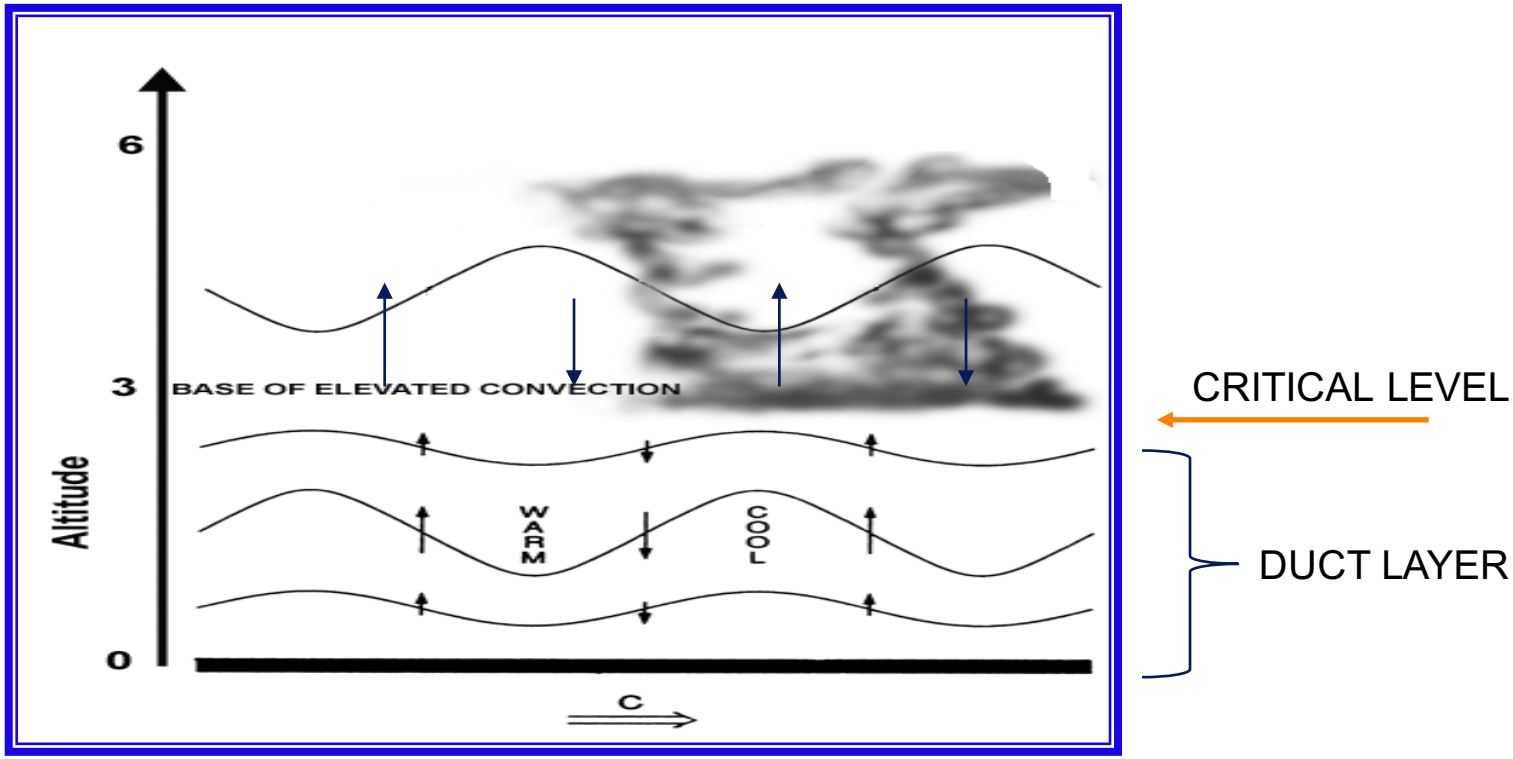

- Waves primarily confined to stably stratified duct layer beneath a critical level with maximum isentropic wave amplitude midway through the duct layer
- Sudden phase shift occurs at the critical level as updrafts change from being 90^0 out of phase with isentropes below this level to being 180^0 out of phase
- Strong updraft at the critical level suggests that model-predicted convection travels in tandem with the gravity wave, as in wave-CISK theory


Thunderstorm Generation by
Bores and Solitons

Evolution of a Density Current into a Bore

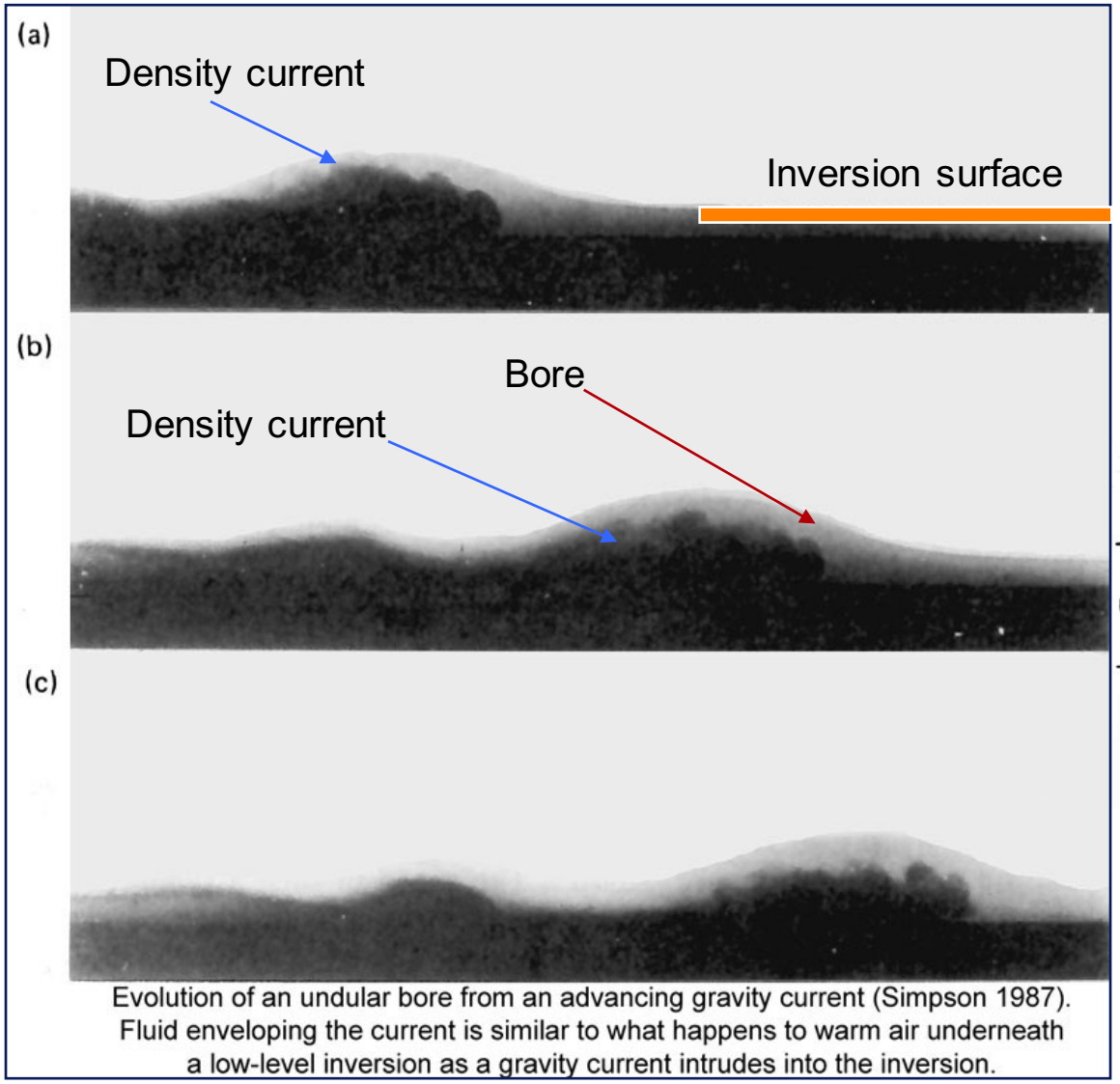

Evolution of an undular bore from an advancing gravity current (Simpson 1987). Fluid enveloping the current is similar to what happens to warm air underneath a low-level inversion as a gravity current intrudes into the inversion.

An internal bore in the atmosphere is a type of gravity wave generated by the intrusion of a density current into a ground-based stable layer. The density current is most typically produced by cold outflow from active convection.

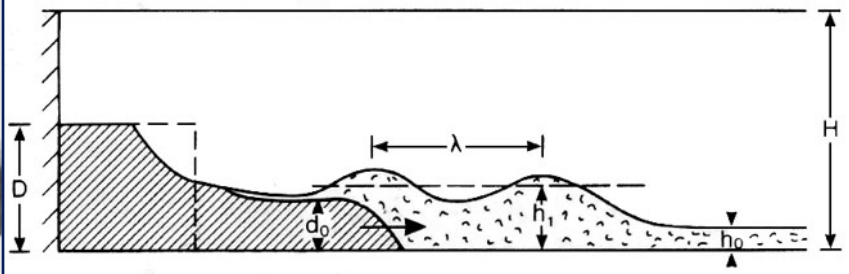

Generation of an internal bore of depth h_1 by an advancing gravity current of depth d_0 intruding into a stable layer of depth h_0

Passage of the bore results in a sustained elevation of the stable layer. Unlike density currents, bores do not transport mass.

Evolution of a Bore into a Soliton

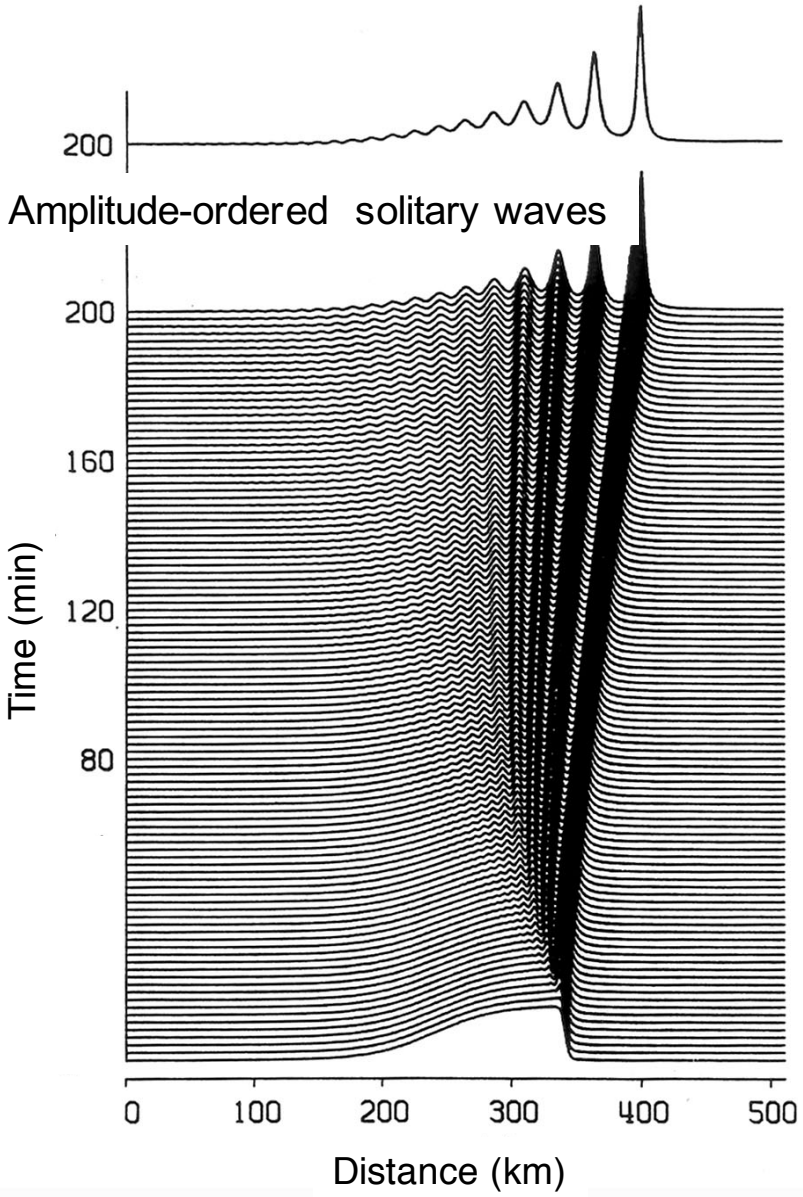

Solution of the BDO equation for deep-fluid solitary waves from an initial wave of elevation along an inversion in a waveguide embedded in a neutrally stable fluid of infinite extent (Christie 1989)

A train of amplitude-ordered solitary waves (or soliton) can evolve from stronger bores in some instances. Wave amplitudes vary inversely with their width.

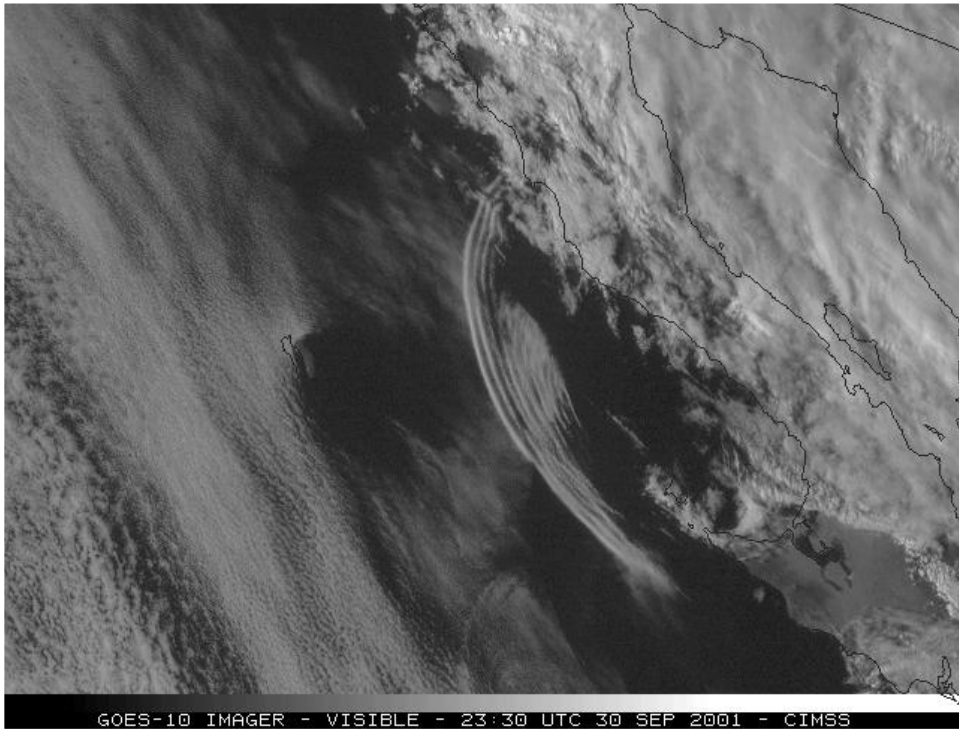

The number of waves increases with time, limited by turbulent dissipation. The energy of the wave system tends to be concentrated in the first few solitary waves.

Undular and Turbulent Bores

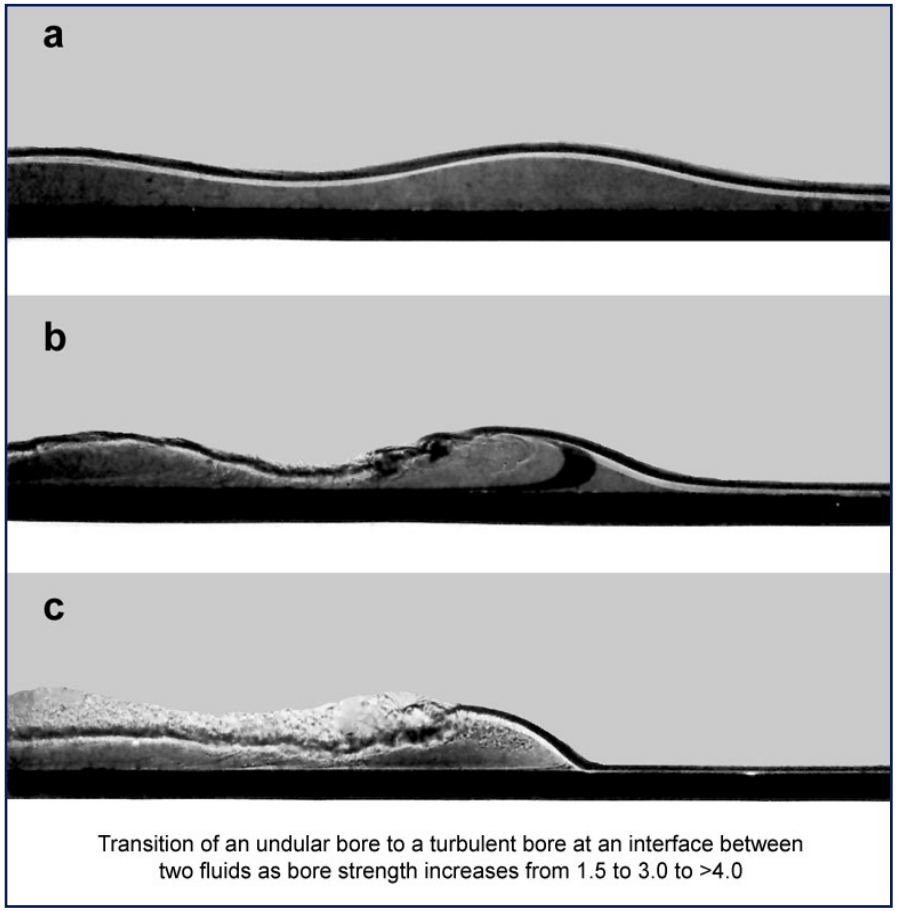

Transition of an undular bore to a turbulent bore at an interface between two fluids as bore strength increases from 1.5 to 3.0 to >4.0

Bore strength (h_1 / h_0) is determined by the Froude Number and the ratio of the density current depth to the inversion depth (d_0 / h_0).

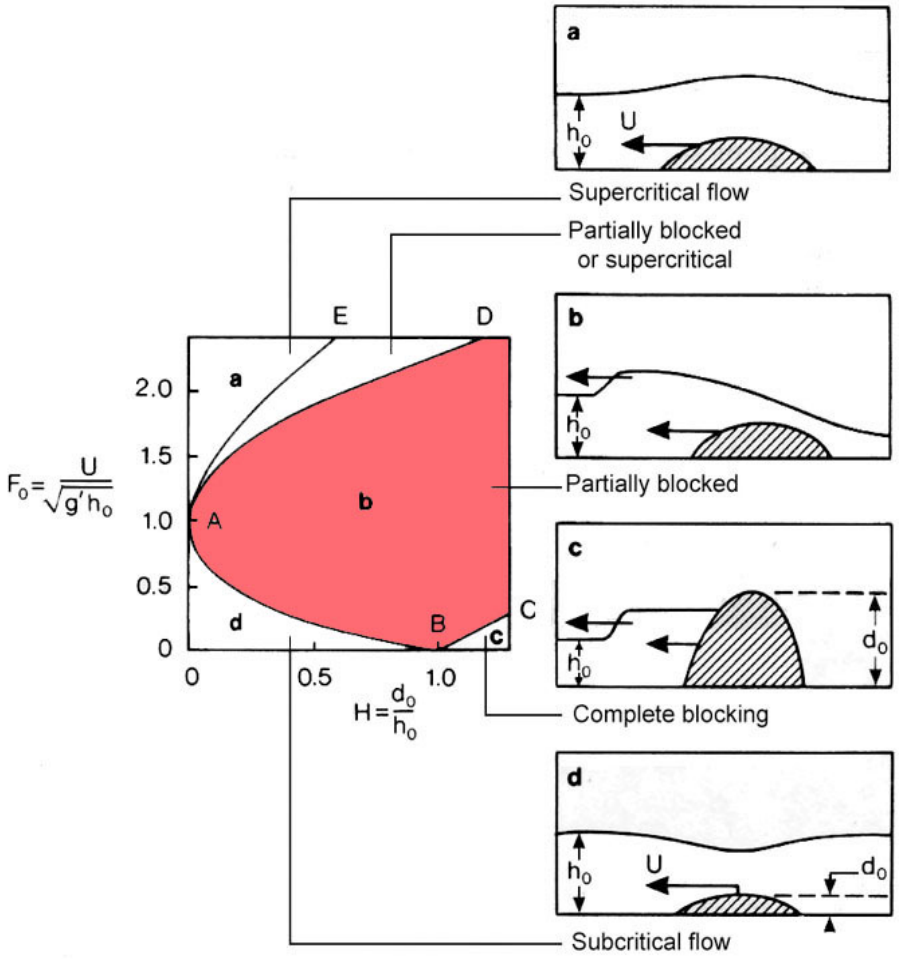

Four types of disturbances that can be generated by a moving obstacle at the interface between two fluids (hydraulic theory)

Stronger bores propagate faster when inversion strong.

$$C_{bore} = C_{gw}\sqrt{0.5\left(d_b/h_0\right)\left(1+d_b/h_0\right)}$$

$$= Nh_0\left[0.5\left(d_b/h_0\right)\left(1+d_b/h_0\right)\right]^{1/2}$$

WAVE DUCTING: Needed to maintain bores

According to the wave dispersion equation, upward propagating (internal) plane waves in the absence of the Coriolis force can only occur if intrinsic frequency $v < N$. Otherwise, they are "evanescent".

$$m^2 = \frac{N_m^2}{(U - C_b)^2} - \frac{\partial^2 U / \partial^2 z}{(U - C_b)} - k^2$$

Consider just the stability term of Scorer parameter:

$$m^2 = \left(\frac{N}{v}\right)^2 k^2 = \left[\frac{N}{k(C - U)}\right]^2 k^2 = \left(\frac{N}{C - U}\right)^2$$

At the "critical level", where $C = U$, the waves are "trapped" from further upward propagation as the vertical wavenumber m becomes infinite.

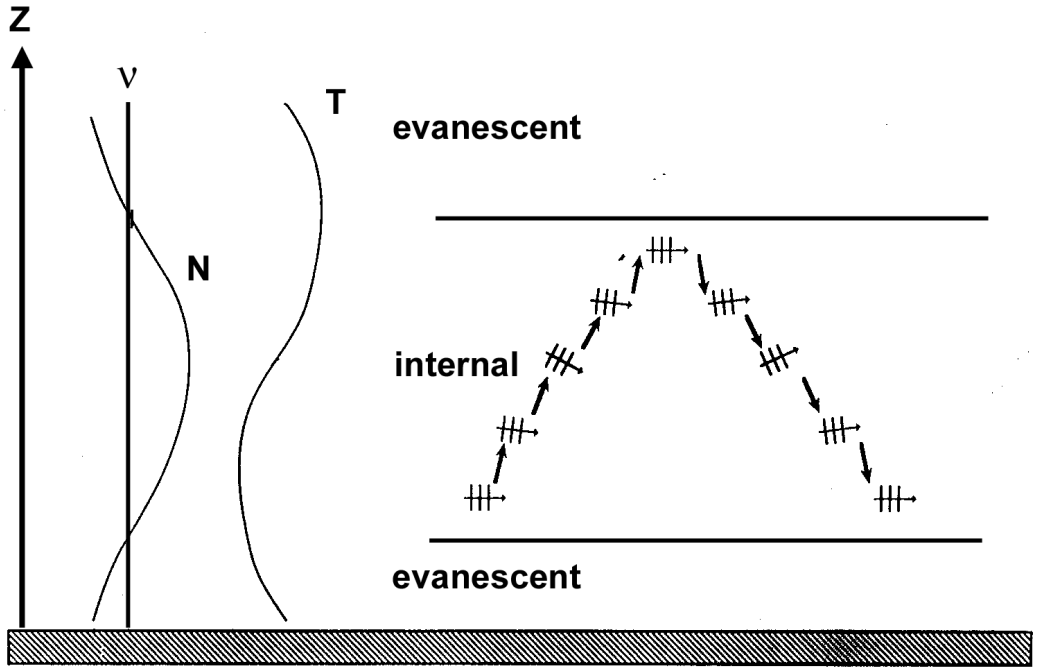

The internal layer represents a "wave duct". However, this stable layer must be thick enough to accommodate 1/4 of the vertical wavelength. Also, at the critical level, the Richardson Number must be small (<0.25).

Remote sensing observations of a bore-soliton system

(Toms, Tomaszewski, Turner, Koch 2016)

Time-Height cross section of bore-normal wind component from Doppler Wind Lidar

Time-Height cross section of vertical motion from Doppler Wind Lidar

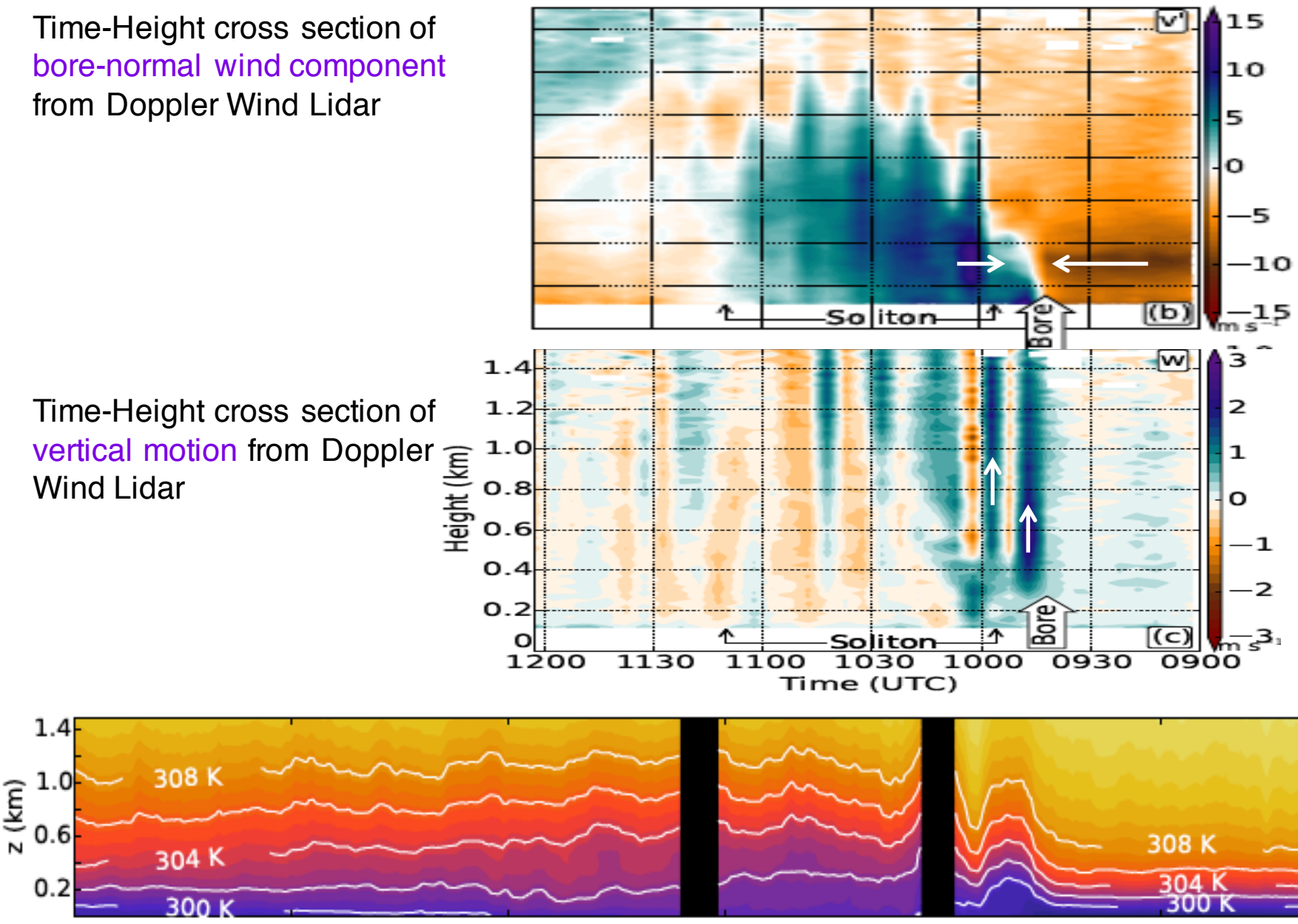

Time-Height cross section of Potential Temperature retrieved from infrared interferometer

Remote sensing observations of a bore-soliton system

(Toms, Tomaszewski, Turner, Koch 2016)

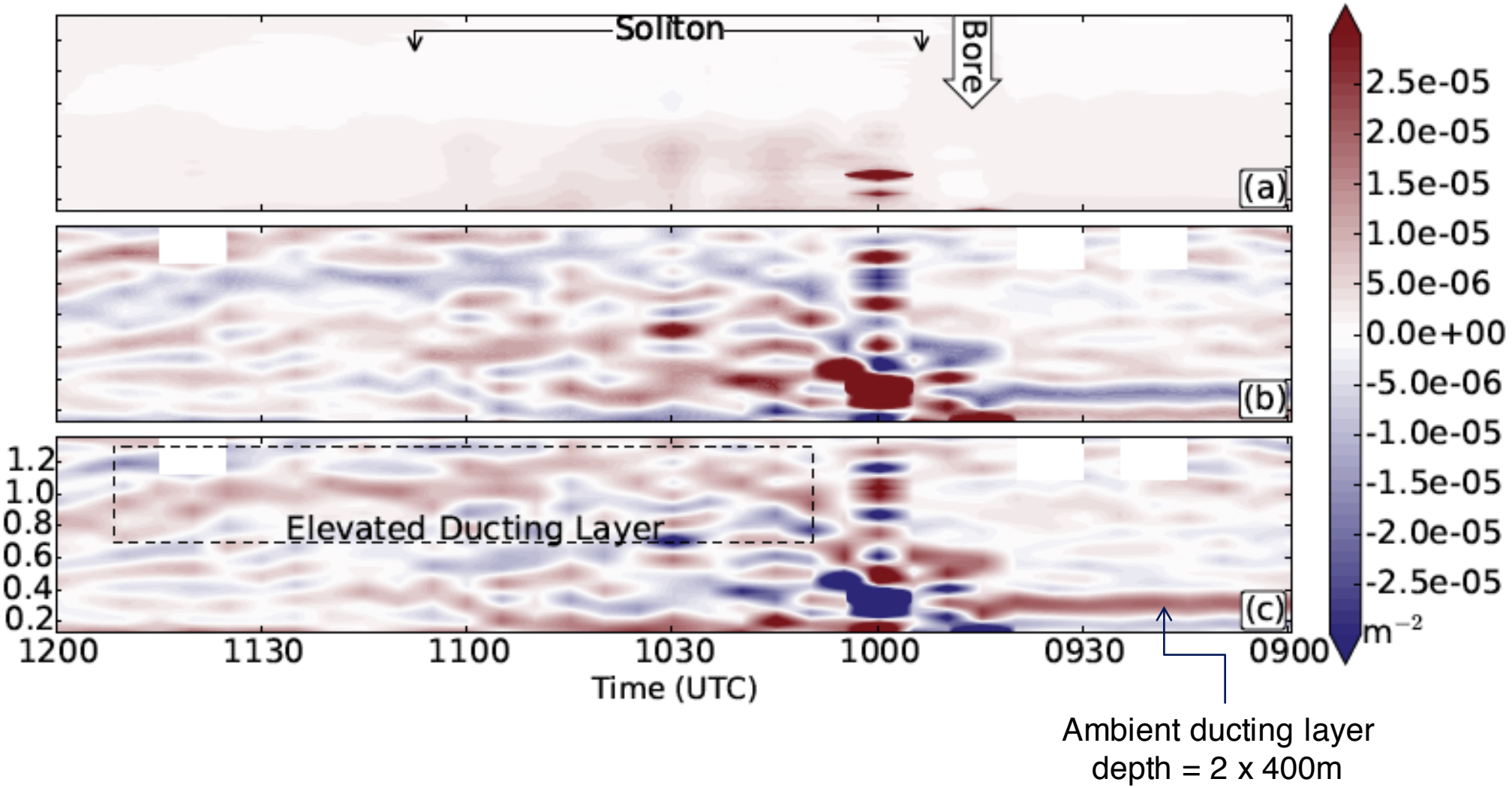

Time-Height cross section of (top) stability and (middle) curvature term of the (bottom) Scorer parameter derived from AERI and DWL data

Observations and Prediction of Convection-Gravity Waves Interactions

Reprinted from MONTHLY WEATHER REVIEW Vol. 103, No. 6, June 1975, pp. 497–513
American Meteorological Society
Printed in U. S. A.

To Steve
many thanks
for your patience
in reading off those
down pressure
readings, all ten
thousand of them

Louis

A Case Study of Apparent Gravity Wave Initiation of Severe Convective Storms

LOUIS W UCCELLINI

Department of Meteorology, University of Wisconsin, Madison, Wis. 53706

(Manuscript received 13 November 1974; in revised form 7 February 1975)

ABSTRACT

A detailed study of an outbreak of severe convective storms is presented which investigates the interaction between subsynoptic scale gravity waves and the convective activity. The gravity waves were isolated by passing digital forms of nearly 130 National Weather Service and FAA barograph traces through a normal weighted band pass filter and then analyzing pressure perturbation (p') fields for the Midwest region at 15-minute intervals. The waves had periods of about 3 h, trace speeds between 35 and 45 m s^{-1} and amplitudes between 0.5 and 2.5 mb. Analyses of surface weather reports, radar data, surface wind convergence, and surface p' fields revealed that the intensity of the convective systems pulsated with periods ranging from 2 to 4 h; and that the gravity waves were a precursor to storm development in Iowa and Wisconsin and appeared to initiate convection in those areas. Reintensification of preexisting storm cells or the development of new cells generally followed the passage of the wave trough, with maximum rainfall intensity coinciding with the passage of the ridge. The cycle is completed with a general weakening of the convective storms as the next trough approaches. To substantiate the proposed causal relationship, the observations were found to be consistent with a theoretical model of subsynoptic scale gravity waves.

Fundamental relationships and equations

$$\hat{u} = \frac{\nu k + i l f}{\rho_0 \left(\nu^2 - f^2\right)} \hat{p}$$

"Polarization relationship": u and p are in-phase when $f = 0$

$$\hat{w} = \frac{\nu\, m}{i\, \rho_0\, N^2} \hat{p}$$

w and p are are in "phase quadrature"

$$C_i = \frac{\nu}{k} = \frac{\hat{p}}{\rho_0 \hat{u}}$$

(the "IMPEDANCE RELATION")

C_i = intrinsic phase speed (=N/m if f=l=0)

$C_p = C_i + U$ = ground-relative phase speed

$$\nu^2 = f^2 + \frac{N^2}{m^2}\left(k^2 + l^2\right)$$

The wave dispersion equation relates wave frequency to stability

CCOPE (1982) and STORM-FEST (1992) studies of interactions between gravity waves and convection:

Use of surface mesonet and digital radar imagery to analyze polarization and wave impedance relations. Also, first ever dual-Doppler retrieval of gravity wave vertical structure compared to predictions from linear stability theory

CCOPE: Convective Feedback Effects on Gravity Waves

(Koch and Golus 1988; Koch et al. 1988; Koch et al. 1992)

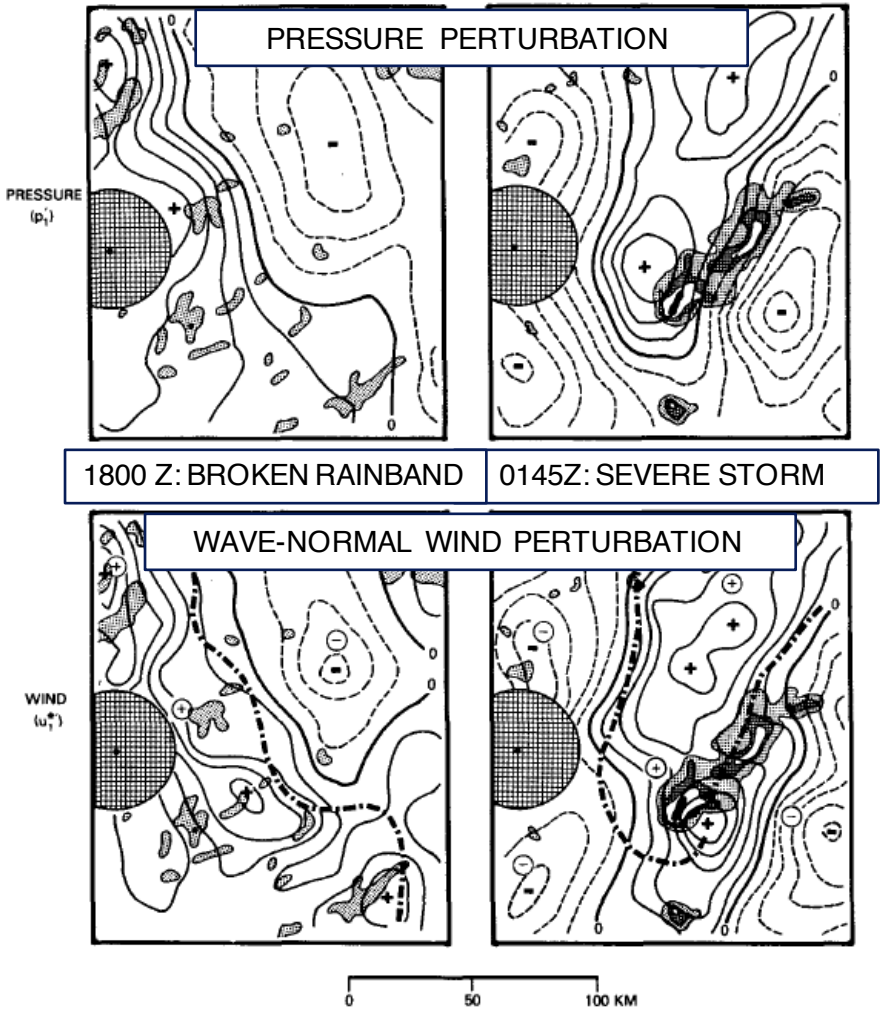

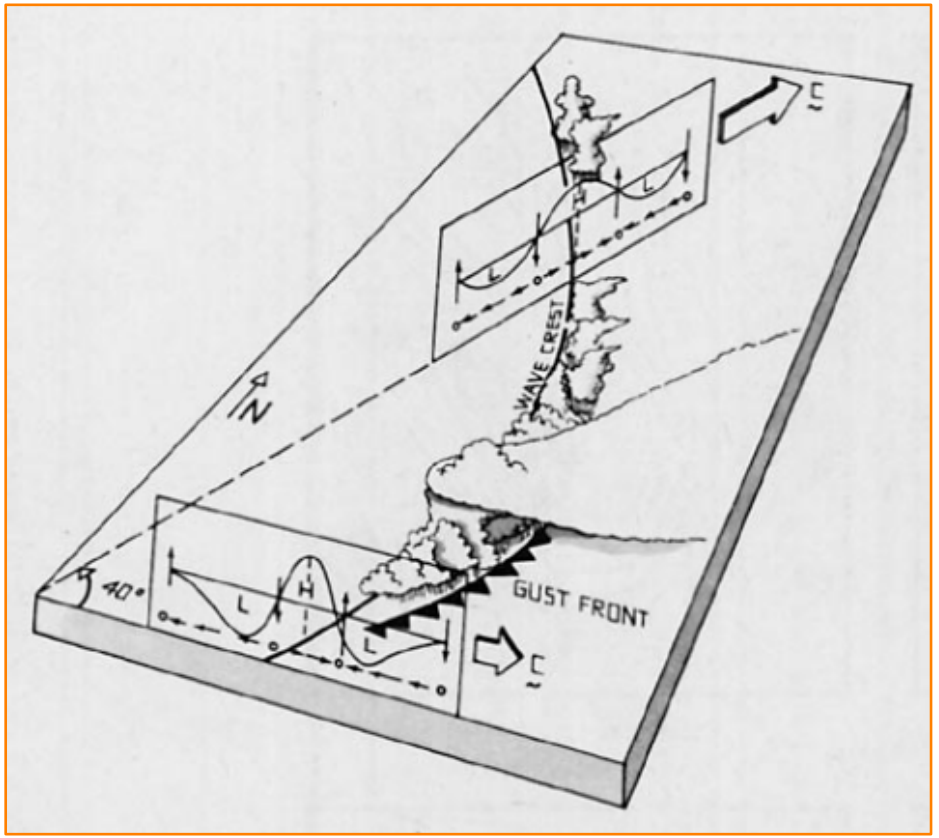

- Strong convection affects waves locally in multiple ways (next slide)
- Original wave signal properties remain intact outside of intense convective cores
- The entire wave-storm system can remain coupled in a synergistic way far downstream
- Note similarity in a sense to the wave-CISK concept

CCOPE: Convective Feedback Effects on Gravity Waves

(Koch et al. 1988)

Observed Convection Feedback Effects on Waves	Cause for Convection Feedback Effects on Waves
Enhanced wave pressure amplitude	Evaporative cooling & latent heating
Nonsinusoidal wave structure in pressure and wave-normal winds and reduced horizontal wavelength	Nonhydrostatic “inflow mesolow”, hydrostatic “bubble mesohigh” and resultant parcel accelerations
Change in propagation velocity (slower and to the right)	Systematic growth of new cells on the right flank of older storm cells
Loss of p’-u’ covariance	Acceleration toward gust front

STORM-FEST: Multi-case analysis of gravity waves

Koch and Siedlarz (1999)

- Bandpass-filtered mesonet data subjected to time-to-space conversion were related to composited satellite and radar reflectivity imagery
- 13 wave events identified, representing 34% of the total hours analyzed
- Wave crests were closely aligned with rainbands throughout their lifetimes.
- The greatest pressure-wind covariance (polarization relation) occurred with the strongest waves.
- Polarization relation diminished during convective intensification stage (F55).
- High covariance restored once the wave-convective system matured into a stable MCS (JH88).

Surface pressure and wind fields associated with mature MCS (Johnson and Hamilton 1988)

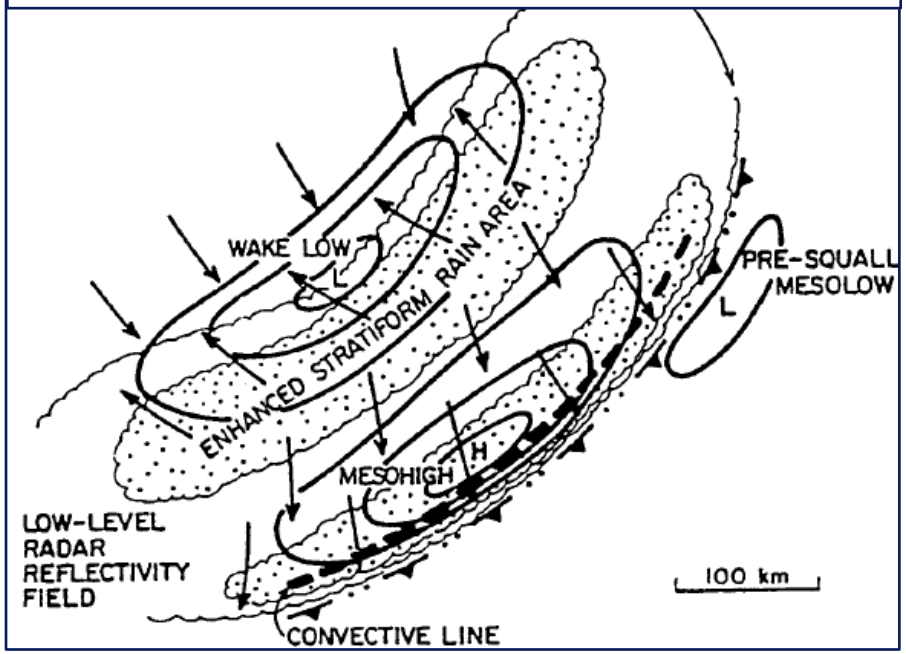

Surface pressure and wind fields associated with thunderstorm (Fujita 1955)

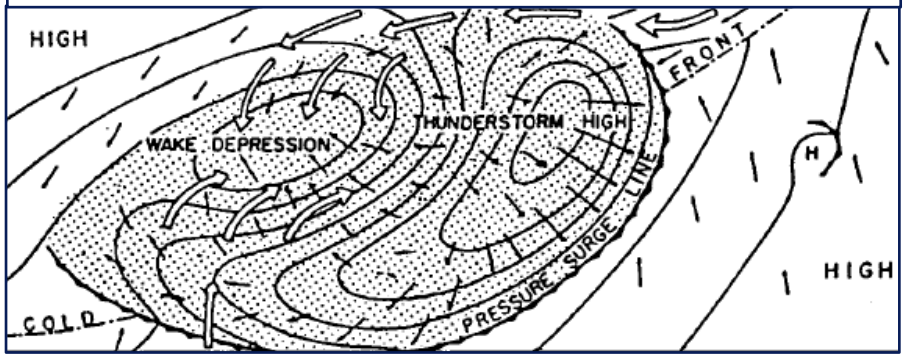

Interactions between gravity waves and convection on 15 December 1987:

First joint use of mesoscale NWP model with detailed mesoanalyses to understand gravity wave nature and genesis mechanisms

Large-Amplitude MGW Event of 15 Dec 1987

Schneider (1990), Powers and Reed (1993), Pokrandt et al. (1996)

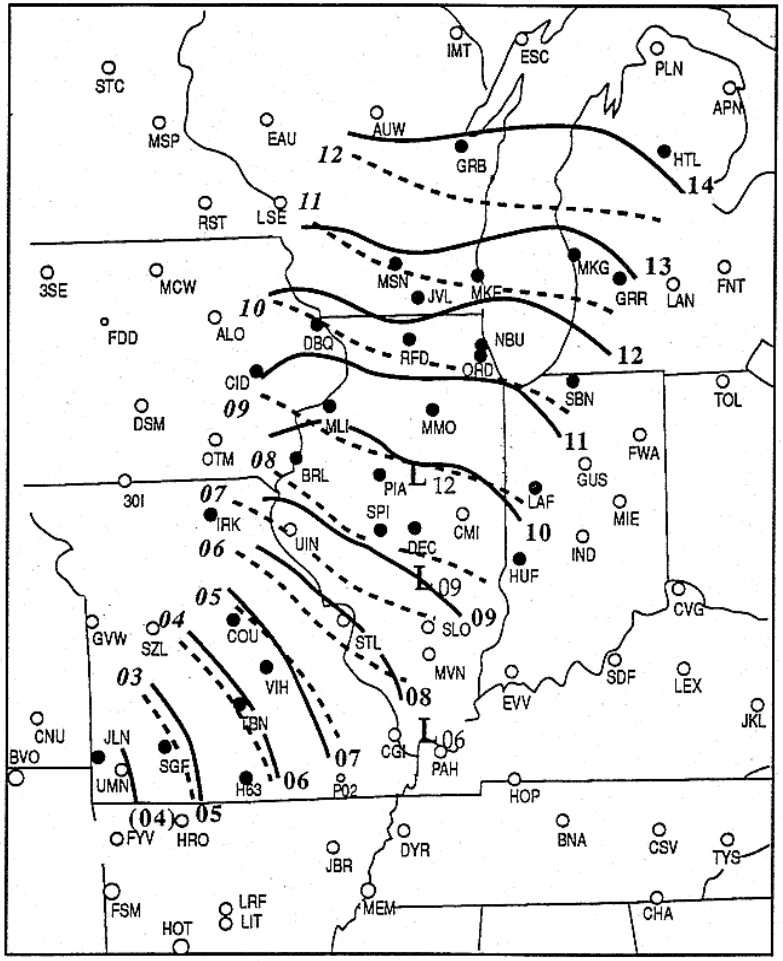

Observed wave isochrones

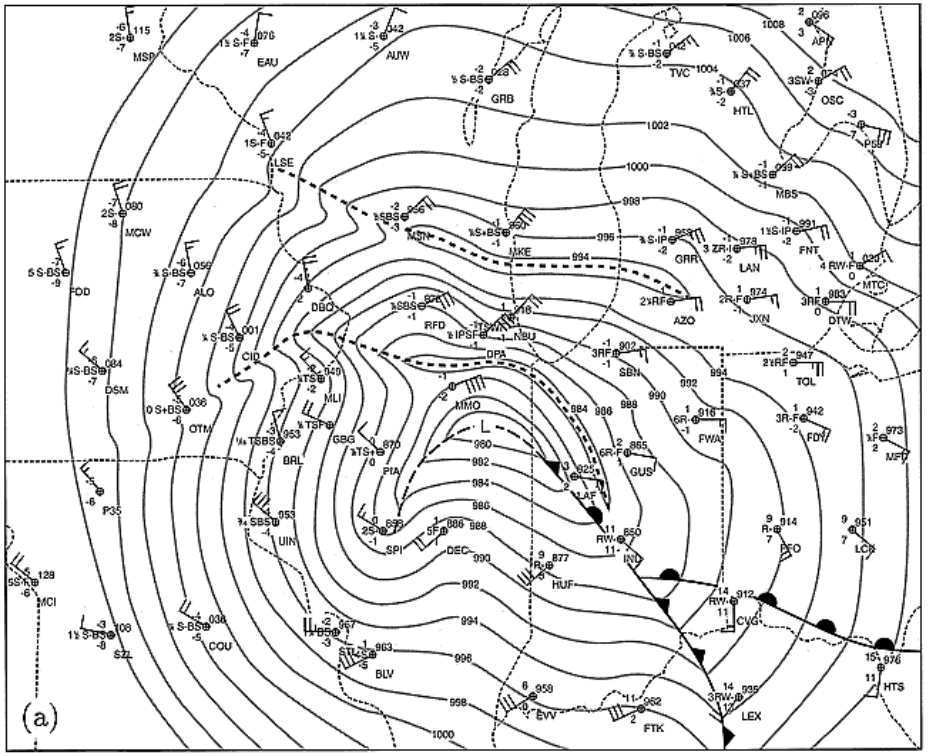

Surface observational analysis

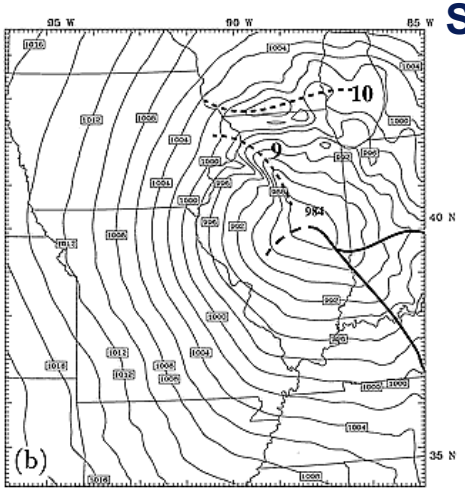

MM5 10-km simulation

1. Simulations improved with higher resolution & more waves generated
2. Ducted Wave-CISK modes suggested by model

The role of convective heating in gravity wave generation and maintenance

(Powers 1997)

Observational analysis at 1100 UTC

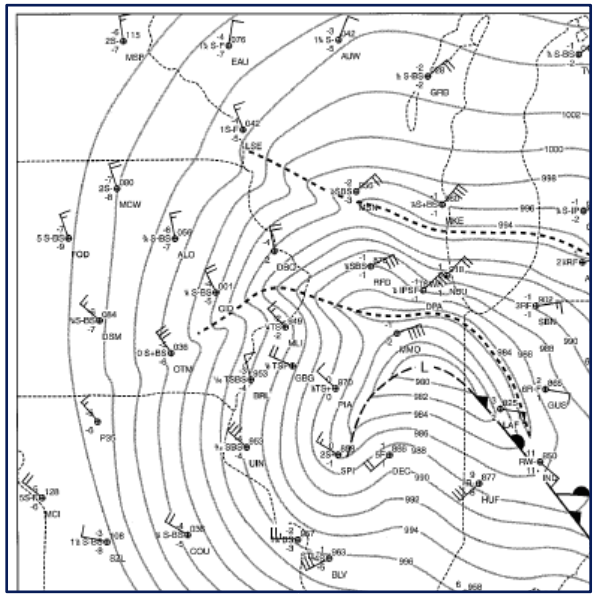

Control simulation at 0400 UTC ⟶ RD simulation at 0800 UTC

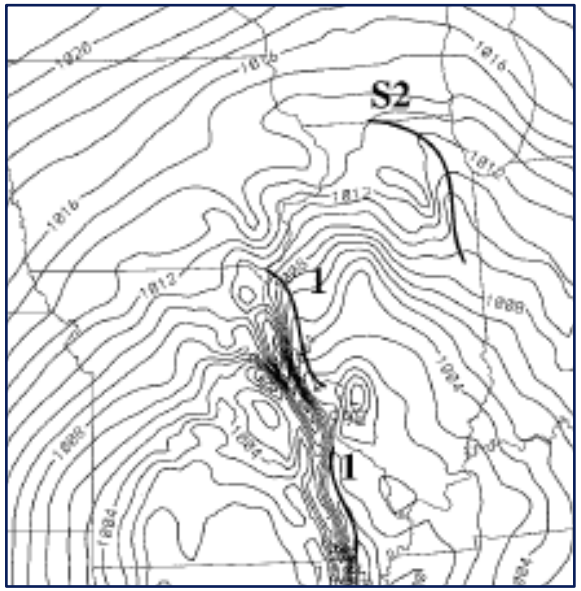

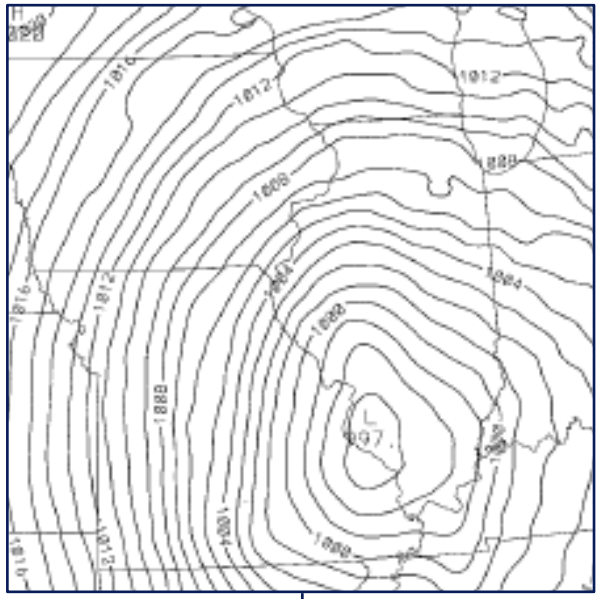

Control simulation for 1100 UTC

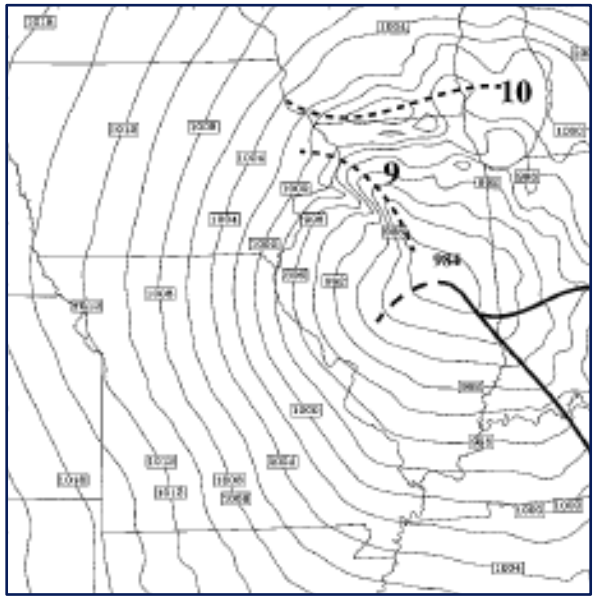

RM simulation at 1200 UTC

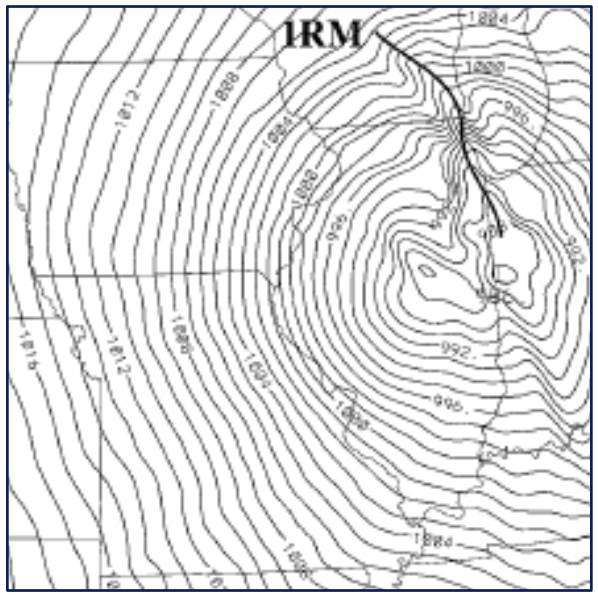

Setting LH to 0 after 4h of full-physics simulation (RD) and restarting the model at 0400 dramatically diminishes the wave activity thereafter.

Reintroduction of LH (RM) at 0800 results in new wave generation and continuance.

Conclusion: latent heating is necessary for development and maintenance of mesoscale gravity waves.

Interactions between gravity waves and convection during the 27 March 1994 tornado outbreak:

First use of automated surface system jointly with mesoscale NWP model for analyzing the polarization relation – ducted wave-CISK modes were quantitatively examined

Band pass filtering of model fields enables identification of gravity waves and positive pressure-wind covariance

(Koch et al. 1998)

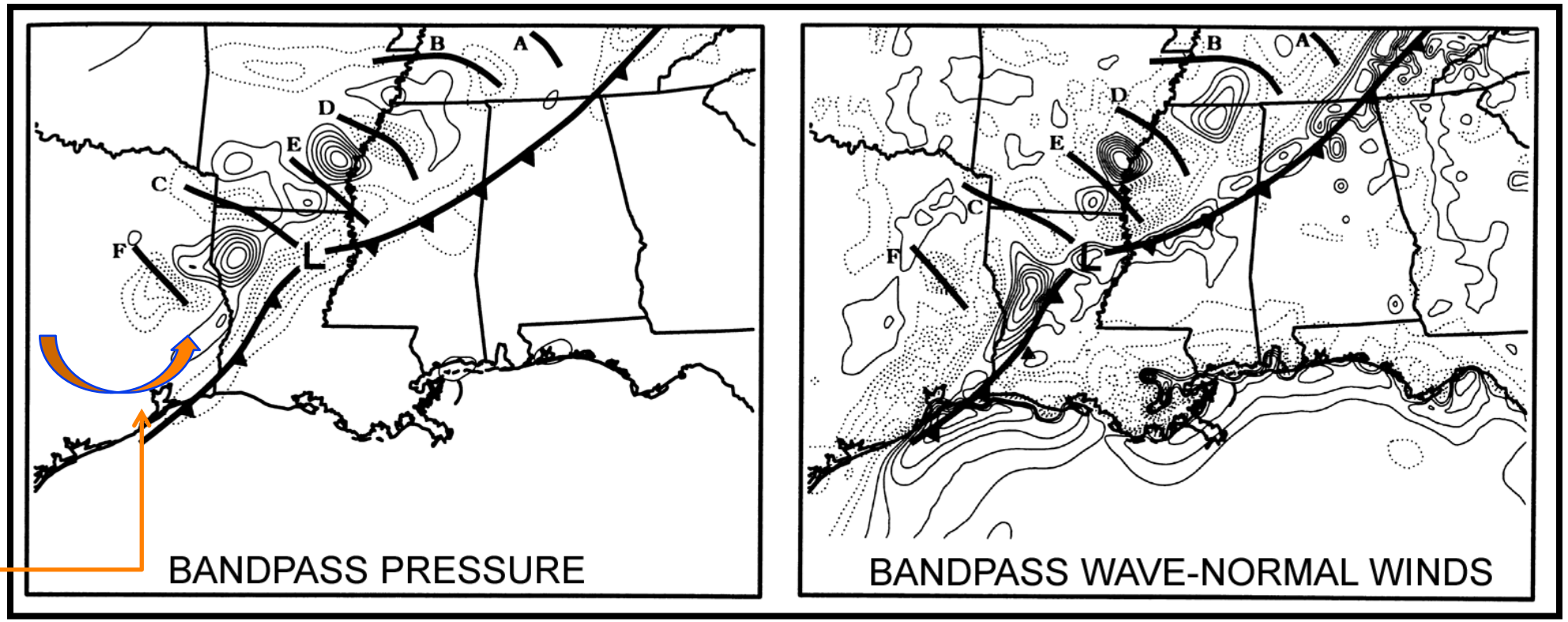

24-km resolution mesoscale NWP model forecast of the 27 March 1994 tornado outbreak

- Train of 150-km wavelength gravity waves just north of the cold front
- Diagnosed as “ducted Wave-CISK modes”
- Wave train traced back, and remained coupled, to an unbalanced “jetlet” forced by earlier convection upstream over Texas.
- The waves helped generate new severe storms in MS-AL

STORMFEST 14 February 1992 Case:

- Bandpass-filtered mesonet observations subjected to time-to-space conversion using wave phase velocity as advection velocity to enhance detail & coherence
- Composited satellite and radar reflectivity imagery
- First joint use of Wind Profiler and Dual-Doppler radar data to study vertical structure of solitary-like wave of depression associated with strong deep convection

Relationship between gravity waves (band pass-filtered surface pressure data) and evolving rainbands

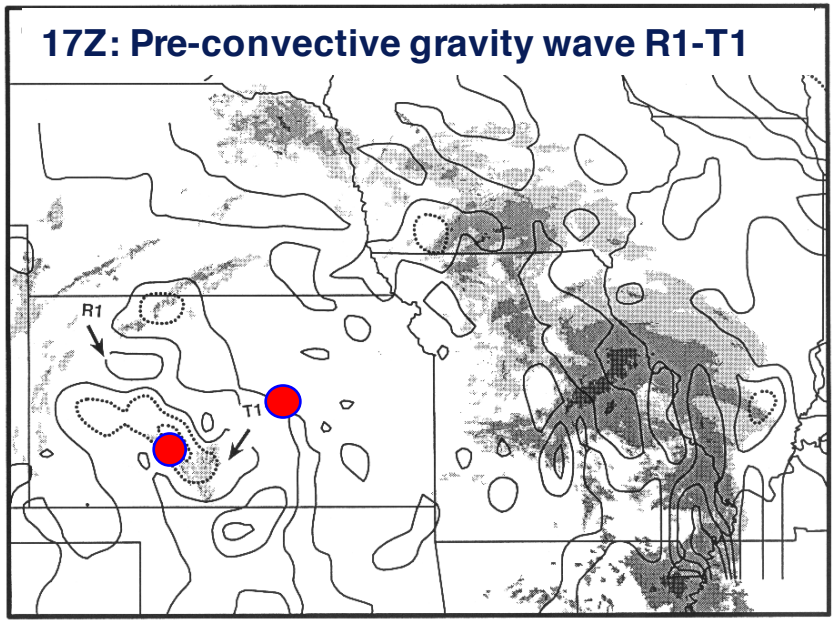

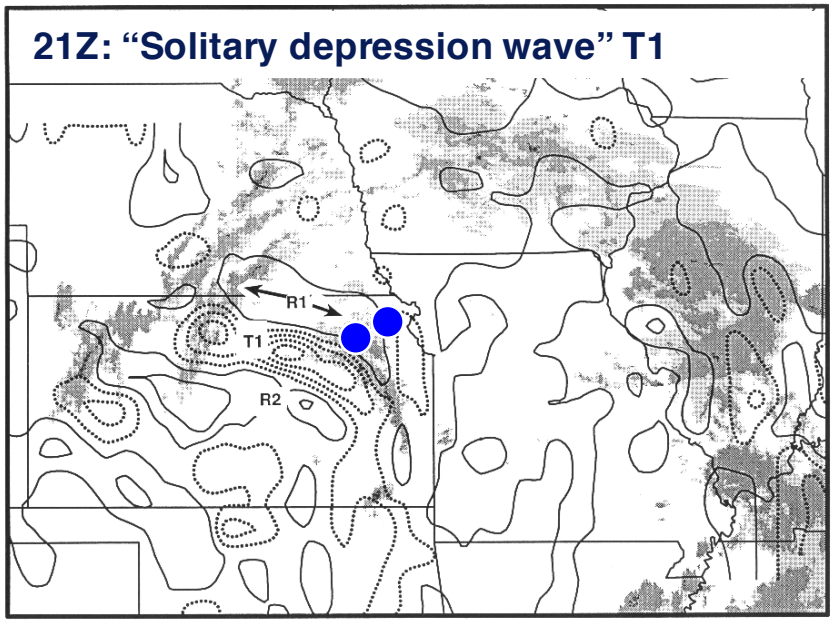

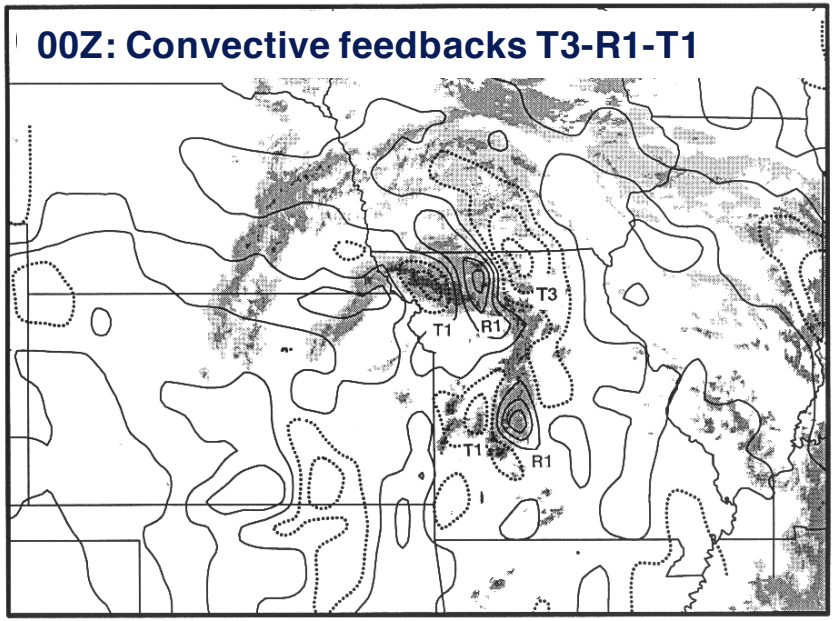

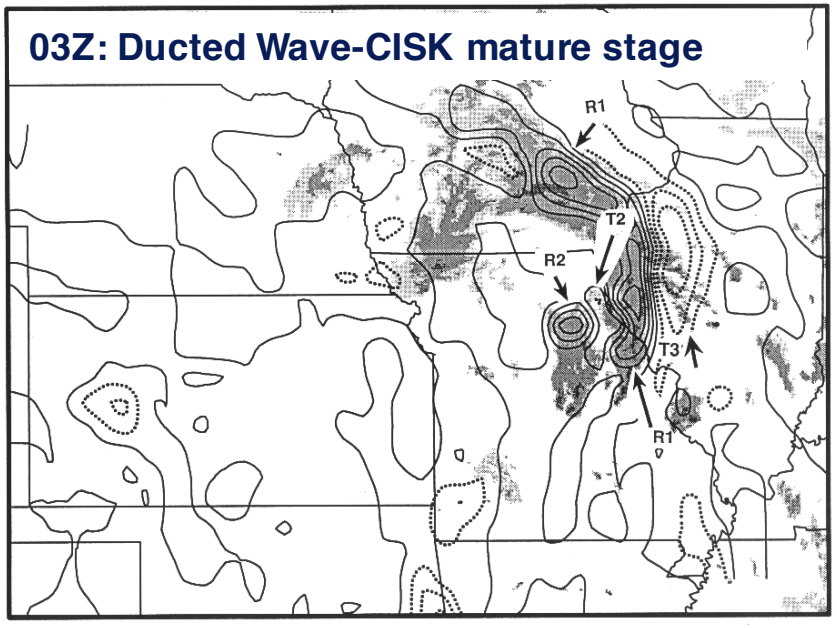

Trexler and Koch (2000) obtained the vertical structure of this gravity wave from an analysis of the NOAA profiler data prior to strong convection (at HVL) and during strong convection (at HBR) (red dots).

Yang et al. (2001) obtained the vertical structure of this gravity wave using STORMFEST Dual-Doppler data near Topeka when the wave-induced convective band was at its strongest (blue dots).

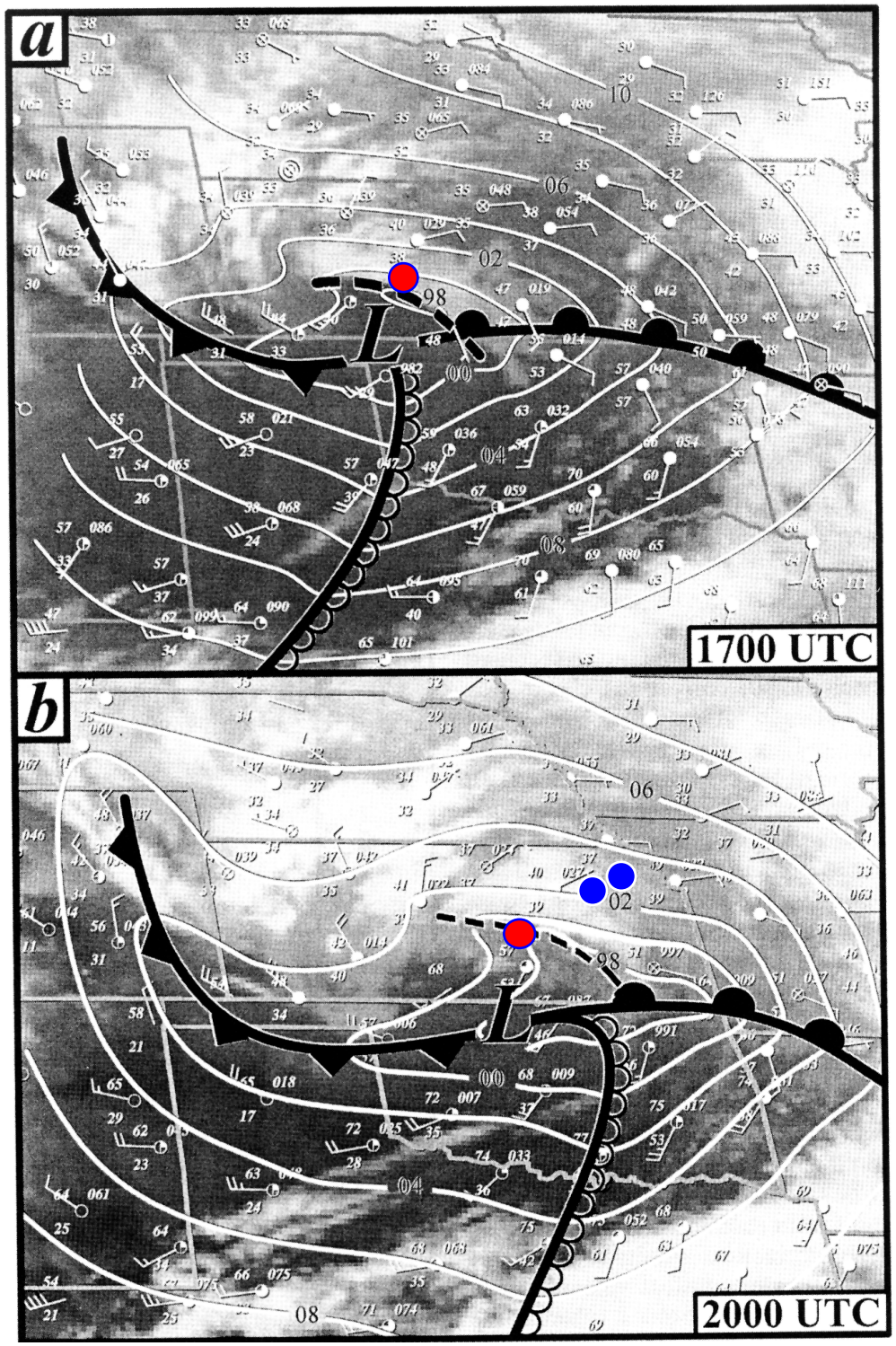

Comparison of evolving gravity wave structures from Wind Profiler and Dual-Doppler Radar analyses

Trexler and Koch (2000)

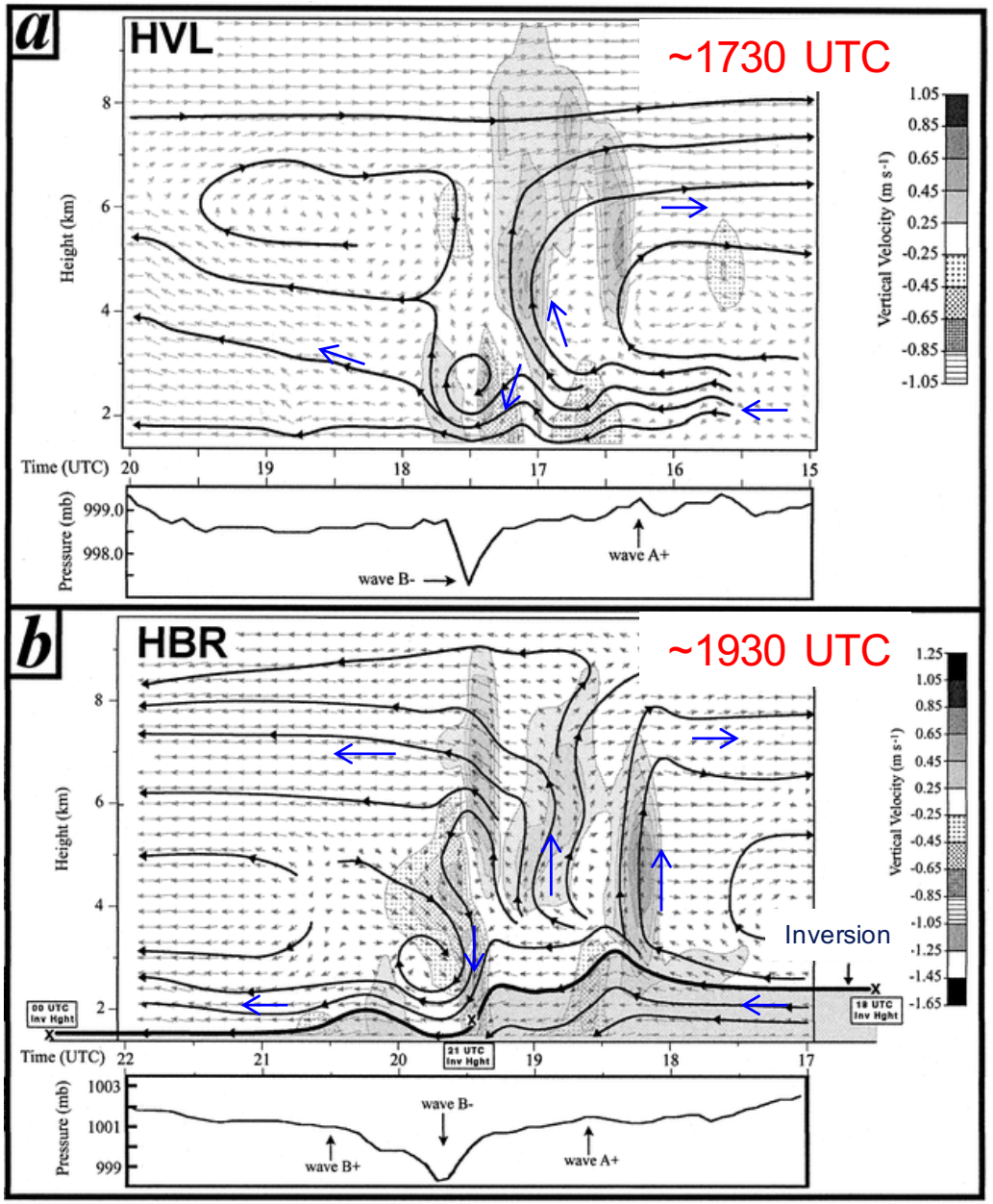

Yang et al. (2001)

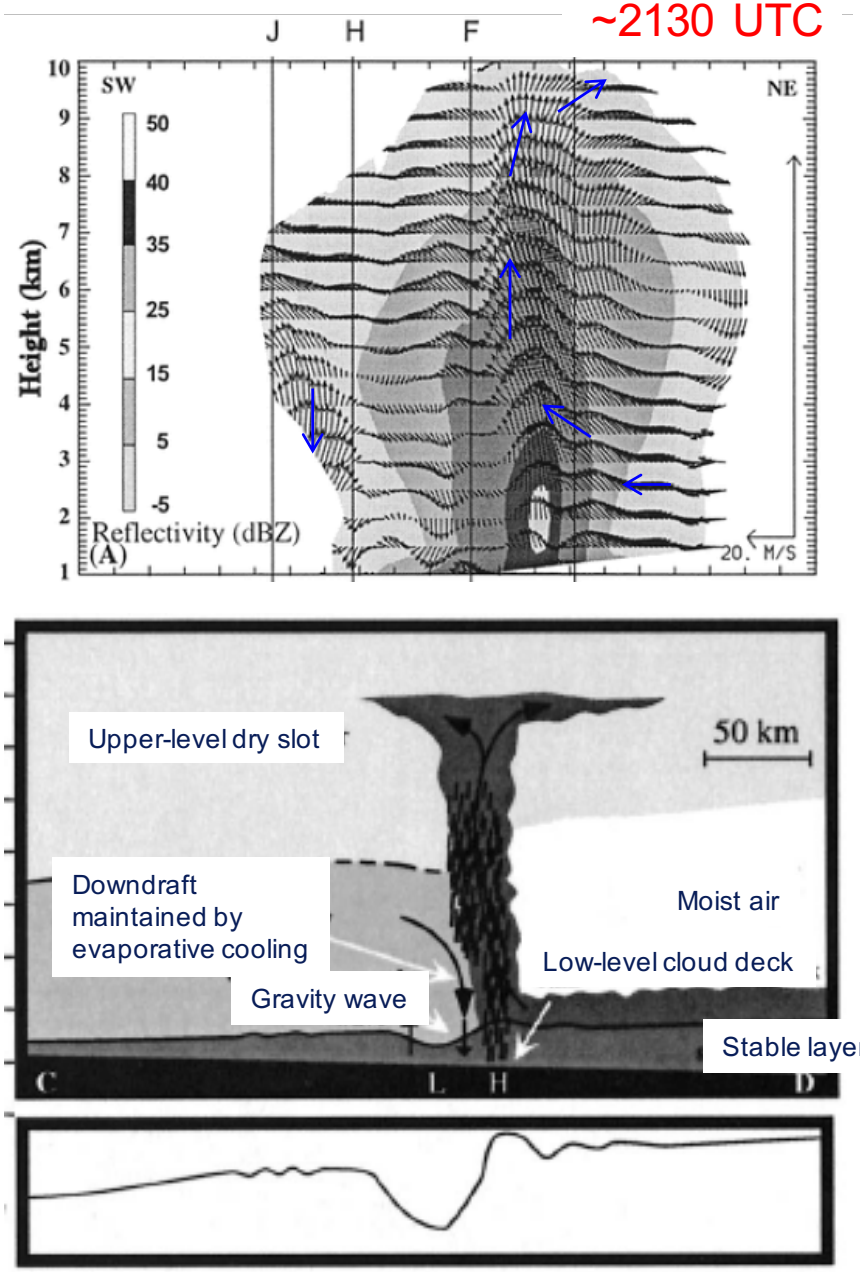

4 January 1994 Case:

Comprehensive high-resolution NWP model sensitivity experiments reveal role of convective latent heating/cooling in gravity wave generation & sustenance

Comparison of 4-km Model Simulation to Observational Analysis

Observational Analysis

Bosart et al. (1998, MWR):

2 GW generated at 0700 Z,
wavelength ~ 100 km,
phase speed ~ 27 m s $^{-1}$,
amplitude ~ 7-8 hPa

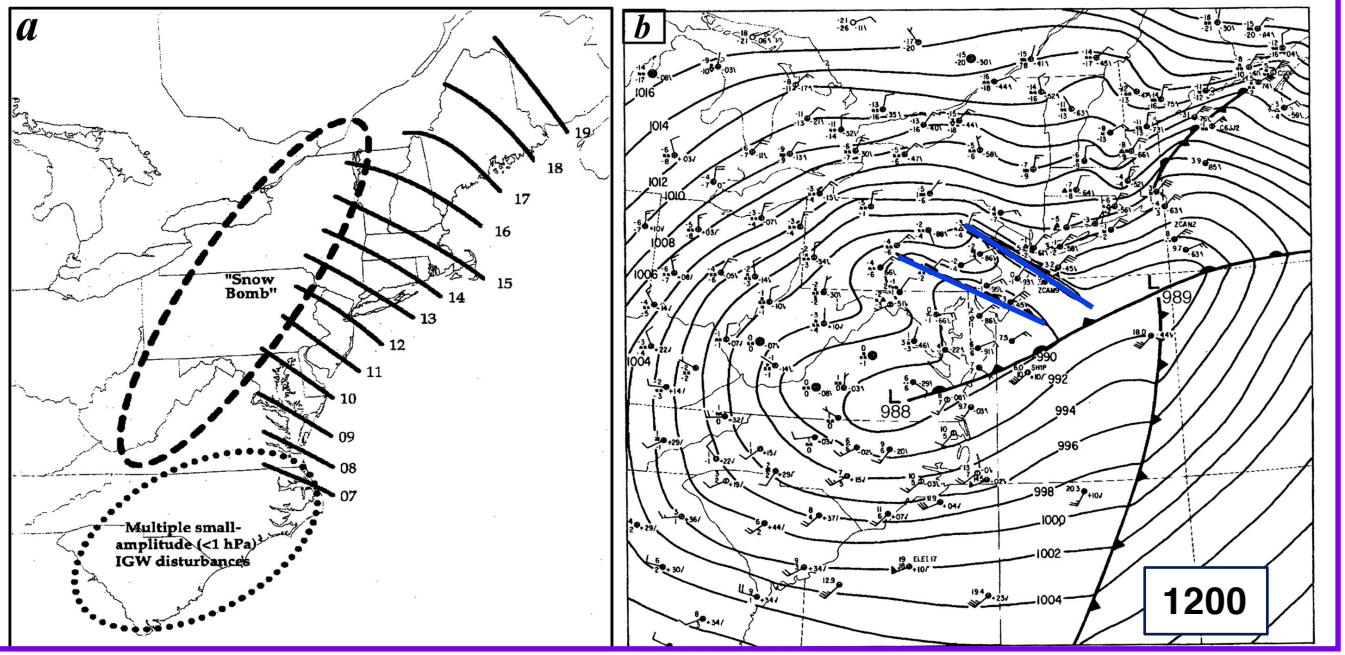

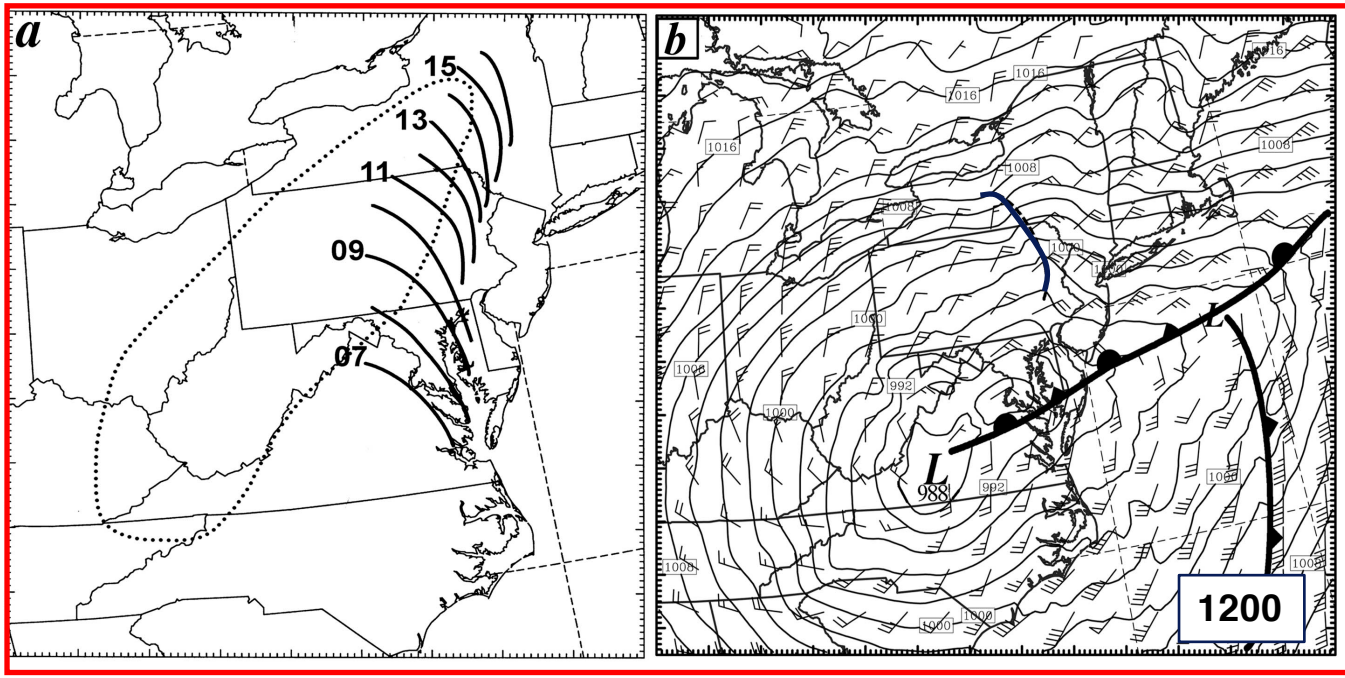

MM5 Model Simulations

Zhang et al. (2001):

1 GW generated at 0700 Z,
wavelength ~ 100 km,
phase speed ~ 25 m s $^{-1}$,
amplitude ~ 3-4 hPa

Sensitivity studies: impact of turning off latent heating/cooling on gravity wave maintenance and evolution

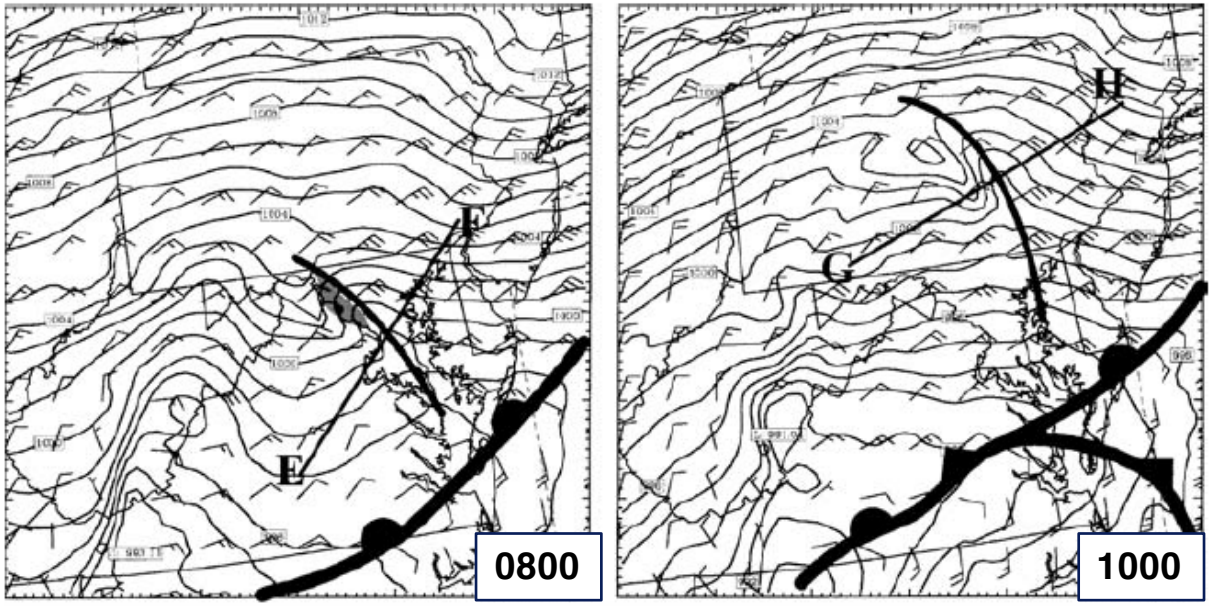

Control run: as in previous slide except at earlier times

Shutting off LH at 0600, 1h ***before*** GW appeared, results in wave demise within 2h

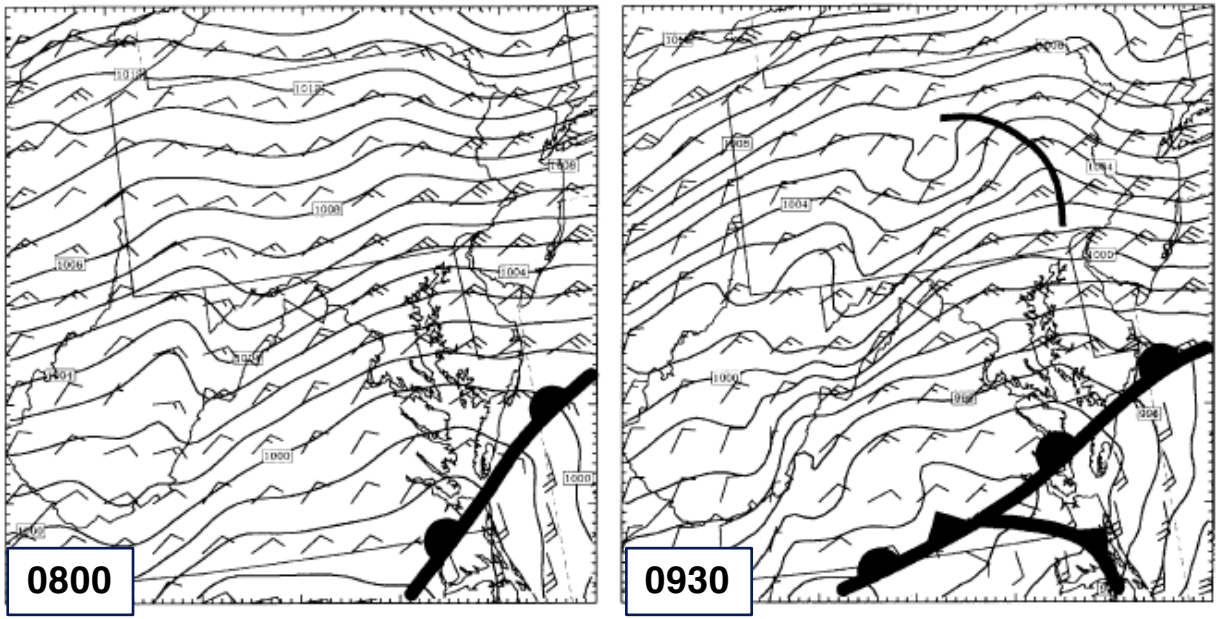

Shutting off LH at 0800, 1h ***after*** GW appeared, results in temporary wave sustenance

Conclusion: Wave-CISK was essential to wave maintenance and amplification

A Methodology for Predicting & Detecting Gravity Waves

- Real-time analysis of mesoscale gravity waves is feasible – provided digital 5-min mesonet data is available
- Prediction begins with recognition of the existence of a jet streak approaching an upper-level ridge axis north of a frontal boundary
- Wave alert region is then refined with diagnosis of flow imbalance and ducting strength computed from mesoscale models. Wave amplitude is highly correlated with strength of convection and wave phase speeds typically match those computed from ducting theory.
- Analysis of observed waves is done with time-to-space (TSC) objective analysis of bandpass filtered 5-min mesonet data
- Wave vertical structure can be deduced from VAD winds and mesoscale model fields

GRID-DEPENDENT WAVELENGTH

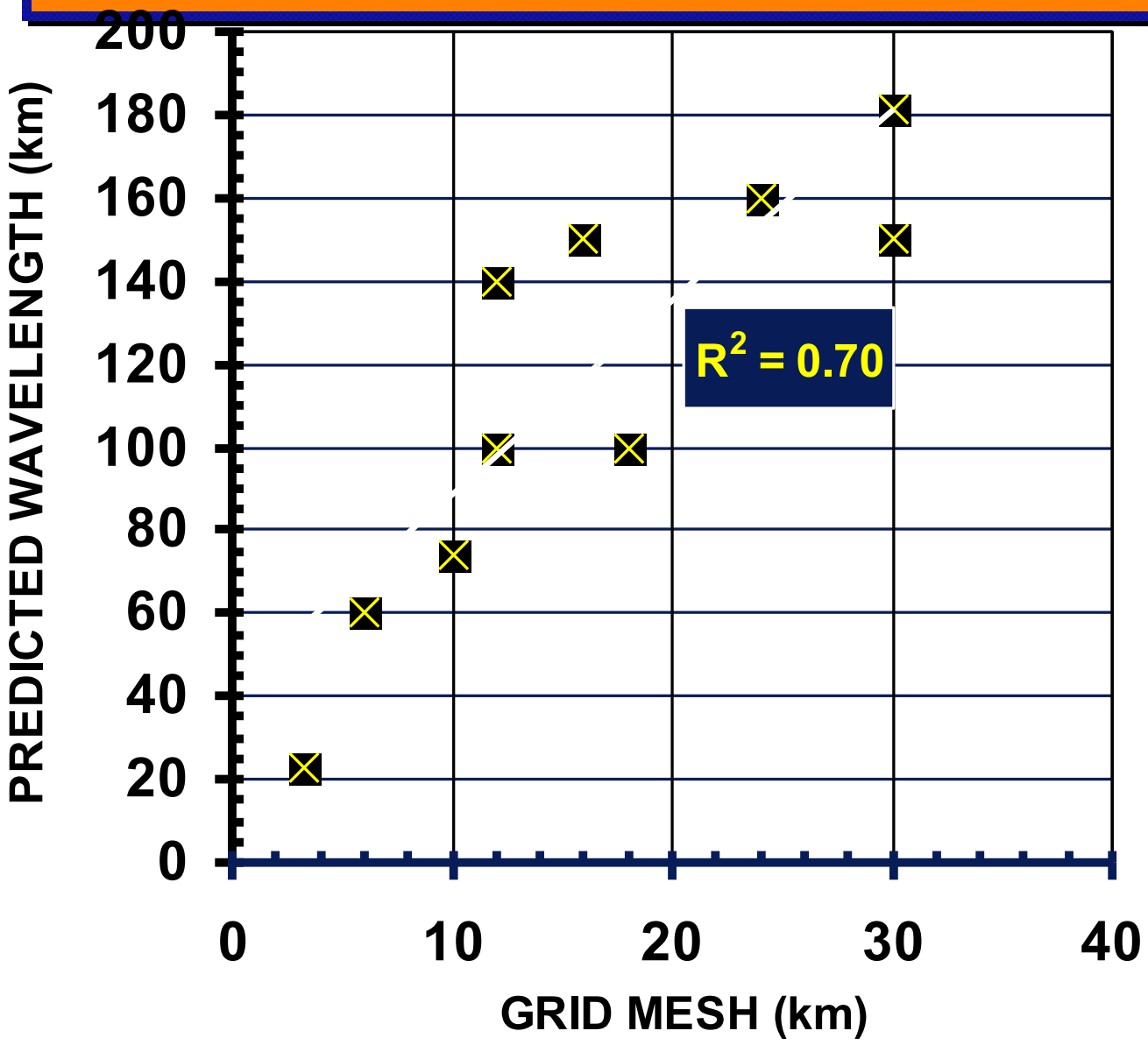

A method for ranking the likelihood of long-lived internal bores based on theoretical and empirical results

(Koch and Haghi 2015)